that type 2 diabetes increases the risk of developing HCC in those who are HCV negative or have a high level of total cholesterol [26]. Second, Nakano et al. reported that epidemiological studies on diabetes mellitus revealed that the number of patients with diabetes mellitus is gradually increasing in Japan along with development of car society and westernization of food intake. Since prevalence of diabetes mellitus increases with aging, proportion of individuals with diabetes mellitus aged over 60 has exceeded two-third of estimated total number of patients (7.40 million in 2002) in Japan where aging of society is rapidly progressing [27]. In a word, the number of type 2 diabetes people is increasing in Japan and they were regarded as a high risk for HCC. Then, the number and the proportion of HCC patients with nonBC have been increased recent twelve years in Japan.

It is known that 2 to 4 decades of chronic HCV infection are required to develop cirrhosis and subsequent HCC [28–31]. The number of HCC cases has increased in Japan, because individuals infected with HCV during the past have grown old and have reached the cancer-bearing age. The prevalence of HCV infection in young Japanese individuals is low and the incidence of HCVAb is very low because of preventative actions against HCV infection such as the screening of blood products for HCV and the use of sterile medical equipment [32]. Additionally, we showed that the number and proportion of patients with HCC-C cases decreased, whereas the number and ratio of HCC-nonBC steadily increased during the studied period. These findings may be expected that the incidence of HCC patients with nonBC in Japan may continue to increase even after the consequence of the HCV epidemic level off, a country that is far advanced with regard to HCC patients with HCV infection, in the near future.

Conclusions

In summary, HCC patients had increased from 1996 to 2000 and this increase was originated from HCC patients with HCV infection. The number and proportion of HCC patients with HCV infection reached a peak in 2000 and thereafter decreased and became stabilized. The incidence of hepatocellular carcinoma associated with hepatitis C infection decreased after 2001 in Kyushu area. This change was due to the increase in the number and proportion of the HCC not only nonBC patients but also B patients.

References:

1. Umemura T, Kiyosawa K: Epidemiology of hepatocellular carcinoma in Japan. Hepatol Res, 2007; 37(Suppl.2): S95–100
2. El-Serag HB, Rudolph KL: Hepatocellular carcinoma: epidemiology and molecular carcinogenesis. Gastroenterology, 2007; 132: 2557–76
3. Kiyosawa K, Tanaka E: Characteristics of hepatocellular carcinoma in Japan. Oncology, 2002; 62: 5–7
4. McGlynn KA, Tsao L, Hsing AW et al: International trends and patterns of primary liver cancer. Int J Cancer, 2001; 94: 290–96
5. Bosch FX, Ribes J, Diaz M, Cleries R: Primary liver cancer: worldwide incidence and trends. Gastroenterology, 2004; 127: S5–16
6. Hamasaki K, Nakata K, Tsutsumi T et al: Changes in the prevalence of hepatitis B and C infection in patients with hepatocellular carcinoma in the Nagasaki Prefecture, Japan. J Med Virol, 1993; 40: 146–49
7. Kato Y, Nakata K, Omagari K et al: Risk of hepatocellular carcinoma in patients with cirrhosis in Japan. Analysis of infectious hepatitis viruses. Cancer, 1994; 74: 2234–38
8. Shiratori Y, Shiina S, Imamura M et al: Characteristic difference of hepatocellular carcinoma between hepatitis B- and C- viral infection in Japan. Hepatology, 1995; 22: 1027–33
9. Shiratori Y, Shiina S, Zhang PY et al: Does dual infection by hepatitis B and C viruses play an important role in the pathogenesis of hepatocellular carcinoma in Japan? Cancer, 1997; 80: 2060–67
10. Kiyosawa K, Umemura T, Ichijo T et al: Hepatocellular carcinoma: recent trends in Japan. Gastroenterology, 2004; 127: S17–26
11. Taura N, Yatsuhashi H, Hamasaki K et al: Increasing hepatitis C virus-associated hepatocellular carcinoma mortality and aging: Long term trends in Japan. Hepatol Res, 2006; 34: 130–34
12. Taura N, Hamasaki K, Nakao K et al: Aging of patients with hepatitis C virus-associated hepatocellular carcinoma: long-term trends in Japan. Oncol Rep, 2006; 16: 837–43
13. Nishiguchi S, Kuroki T, Nakatani S et al: Randomised trial of effects of interferon-alpha on incidence of hepatocellular carcinoma in chronic active hepatitis C with cirrhosis. Lancet, 1995; 346: 1051–55
14. Nishiguchi S, Shiomi S, Nakatani S et al: Prevention of hepatocellular carcinoma in patients with chronic active hepatitis C and cirrhosis. Lancet, 2001; 357: 196–97
15. Kasahara A, Hayashi N, Mochizuki K et al: Risk factors for hepatocellular carcinoma and its incidence after interferon treatment in patients with chronic hepatitis C. Osaka Liver Disease Study Group. Hepatology, 1998; 27: 1394–402
16. Ikeda K, Saitoh S, Arase Y et al: Effect of interferon therapy on hepatocellular carcinogenesis in patients with chronic hepatitis type C: A long-term observation study of 1,643 patients using statistical bias correction with proportional hazard analysis. Hepatology, 1999; 29: 1124–30
17. Makiyama A, Itoh Y, Kasahara A et al: Characteristics of patients with chronic hepatitis C who develop hepatocellular carcinoma after a sustained response to interferon therapy. Cancer, 2004; 101: 1616–22
18. Muto Y, Sato S, Watanabe A et al: Effects of oral branched-chain amino acid granules on event-free survival in patients with liver cirrhosis. Clin Gastroenterol Hepatol, 2005; 3: 705–13
19. Yoshizawa H: Hepatocellular carcinoma associated with hepatitis C virus infection in Japan: projection to other countries in the foreseeable future. Oncology, 2002; 62: 8–17
20. Orito E, Mizokami M: Hepatitis B virus genotypes and hepatocellular carcinoma in Japan. Intervirology, 2003; 46: 408–12
21. Orito E, Mizokami M: Differences of HBV genotypes and hepatocellular carcinoma in Asian countries. Hepatol Res, 2007; 37: S33–35
22. Matsumoto A, Tanaka E, Rokuhara A et al: Efficacy of lamivudine for preventing hepatocellular carcinoma in chronic. Hepatol Res, 2005; 32(3): 173–84
23. Xu J, Shi J, Wang YP et al: Milder liver cirrhosis and loss of serum HBeAg do not imply lower risk for. Med Sci Monit, 2009; 15(6): CR274–79
24. Hayashi N, Takehara T: Antiviral therapy for chronic hepatitis C: past, present, and future. J Gastroenterol, 2006; 41(1): 17–27
25. Kumashiro R, Kuwahara R, Ide T et al: Subclones of drug-resistant hepatitis B virus mutants and the outcome of breakthrough hepatitis in patients treated with lamivudine. Intervirology, 2003; 46(6): 350–54
26. Lai MS, Hsieh MS, Chiu YH, Chen TH: Type 2 diabetes and hepatocellular carcinoma: A cohort study in high prevalence area of hepatitis virus infection. Hepatology, 2006; 43: 1295–302
27. Nakano T, Ito H: Epidemiology of diabetes mellitus in old age in Japan. Diabetes Res Clin Pract, 2007; 77(Suppl.1): S76–81
28. Deuffic S, Poynard T, Valleron AJ: Correlation between hepatitis C virus prevalence and hepatocellular carcinoma mortality in Europe. J Viral Hepat, 1999; 6: 411–13
29. El-Serag HB, Mason AC: Rising incidence of hepatocellular carcinoma in the United States. N Engl J Med, 1999; 340: 745–50
30. Planas R, Balleste B, Antonio Alvarez M et al: Natural history of decompensated hepatitis C virus-related cirrhosis. A study of 200 patients. J Hepatol, 2004; 40: 823–30
31. Davila JA, Morgan RO, Shaib Y et al: Hepatitis C infection and the increasing incidence of hepatocellular carcinoma: a population-based study. Gastroenterology, 2004; 127: 1372–80
32. Sasaki F, Tanaka J, Moriya T et al: Very low incidence rates of community-acquired hepatitis C virus infection in company employees, long-term inpatients, and blood donors in Japan. J Epidemiol, 1996; 6: 198–203

Contrast-Enhanced Ultrasound With Perflubutane Microbubble Agent: Evaluation of Differentiation of Hepatocellular Carcinoma

Masanori Takahashi[1]
Hitoshi Maruyama
Hiroyuki Ishibashi
Masaharu Yoshikawa
Osamu Yokosuka

OBJECTIVE. The aim of this study was to evaluate the effectiveness of contrast-enhanced ultrasound with a perflubutane microbubble agent in the assessment of cellular differentiation of hepatocellular carcinoma (HCC).

SUBJECTS AND METHODS. Continuous harmonic imaging with a low mechanical index (0.21–0.30) was performed 1, 5, and 10 minutes after IV contrast injection (0.0075 mL/kg). Tumor enhancement was evaluated by both subjective reading and objective intensity analysis based on the signal distribution in the nontumor parenchyma. Tumor vascularity was assessed with CT during hepatic arteriography.

RESULTS. Sixty-four patients with 77 histologically proved HCCs (mean greatest dimension, 19.1 ± 5.3 mm)—six poorly differentiated HCCs, 45 moderately differentiated HCCs, and 26 well-differentiated HCCs—were enrolled in this prospective study. Among 64 hyperenhancing lesions on peak enhancement sonograms, four poorly differentiated HCCs and eight moderately differentiated HCCs exhibited washout within 1 minute. In addition to these 12 lesions, 36 lesions exhibited washout 5 minutes after injection, resulting in a total of 48 washout lesions. Fifty-four lesions exhibited washout 10 minutes after contrast injection (six poorly differentiated, 38 moderately differentiated, and 10 well-differentiated HCCs). Washout was more frequent in poorly than in moderately differentiated HCC ($p = 0.0117$) and well-differentiated HCC ($p = 0.0003$) in the 1-minute phase and was more frequent in moderately differentiated than in well-differentiated HCC in the 5-minute ($p = 0.0026$) and 10-minute ($p = 0.0117$) phases. Thirteen lesions were isoenhancing or hypoenhancing on peak enhancement sonograms (three moderately differentiated and 10 well-differentiated HCCs). Contrast-enhanced ultrasound and CT during hepatic arteriography did not differ significantly with respect to rate of detection of hyperenhancing lesions.

CONCLUSION. The findings at contrast-enhanced ultrasound with the perflubutane microbubble agent may be predictive of cellular differentiation of HCC without needle biopsy.

Keywords: cellular differentiation, contrast agent, hepatocellular carcinoma, liver, ultrasound

DOI:10.2214/AJR.10.4242

Received January 5, 2010; accepted after revision July 12, 2010.

[1]All authors: Department of Medicine and Clinical Oncology, Chiba University Graduate School of Medicine, 1-8-1, Inohana, Chuou-ku, Chiba 260-8670, Japan. Address correspondence to H. Maruyama (maru-cib@umin.ac.jp).

WEB
This is a Web exclusive article.

AJR 2011; 196:W123–W131

0361–803X/11/1962–W123

Hepatocellular carcinoma (HCC) is one of the most common forms of cancer worldwide, especially in the eastern part of Asia [1]. Although the results of therapy for HCC have improved remarkably, the prognosis among patients with cirrhosis continues to depend on the rates of occurrence and progression of this tumor [2]. Hypervascularity is a known characteristic imaging finding of HCC [3–6] and an important marker in differential diagnosis. Hypervascularity, however, is a result of dedifferentiation, and some early-stage HCCs appear as isovascular or hypovascular lesions [7–10]. Contrast imaging techniques have become extensively used to assess the vascularization and cellular differentiation of HCC.

With ultrasound, real-time and repeated observation can be performed, and ultrasound is more convenient than CT and MRI. With the development of microbubble contrast agents, the diagnostic utility of ultrasound has increased substantially [11–15]. The perflubutane microbubble ultrasound contrast agent (Sonazoid, GE Healthcare) accumulates in the reticuloendothelial system, such as in the Kupffer cells [16, 17]. As cellular differentiation in HCC progresses from a nontumor tissuelike appearance to well-differentiated cancerous tissue [18–20], the difference in contrast enhancement between the HCC lesion and adjacent liver parenchyma at perflubutane microbubble–enhanced ultrasound may indicate the grade of cellular differentiation of HCC. The results of one study

[21] showed the usefulness of ultrasound enhanced with perflubutane microbubbles in comparison with superparamagnetic iron oxide–enhanced MRI in estimation of the histologic grade of HCC. The results of that study were based on imaging findings represented by accumulation of the microbubbles of the perflubutane agent. However, contrast enhancement may be closely related to the dynamic behavior of the microbubbles while the agent circulates. For this reason, we designed a study to objectively examine phase-related changes in contrast enhancement in signal intensity analysis. The aim of this study was to clarify the clinical efficacy of ultrasound enhanced with perflubutane microbubble contrast material in the noninvasive assessment of cellular differentiation of HCC.

Subjects and Methods

Patients

From February 2007 through September 2009, this prospective study was conducted with the following inclusion criteria: patient has cirrhosis and one or more hepatic lesions smaller than 30 mm in maximum diameter found with unenhanced gray-scale ultrasound, contrast-enhanced ultrasound of the hepatic lesion is scheduled, CT during hepatic arteriography (CTHA) to assess the vascularity of the hepatic lesion is scheduled for less than 2 weeks after the contrast-enhanced ultrasound examination, percutaneous liver biopsy or open resection of the hepatic lesion is scheduled, and the patient has no contraindications to administration of perflubutane microbubble contrast agent, that is, egg allergy and severe pulmonary or cardiac disease. The histologic diagnosis of HCC lesions was made by analysis of the specimen obtained at surgery or ultrasound-guided needle biopsy with a 21-gauge needle (Sonopsy-C1, Hakko) after the contrast-enhanced ultrasound examination. This study was approved by the ethics committee of our institute, and informed written consent was obtained from all patients.

Ultrasound Examination

Ultrasound examinations (SSA-770A or 790A Aplio system, Toshiba) were performed with a 3.75-MHz convex probe. First, unenhanced gray-scale ultrasound imaging (tissue harmonic imaging, 2.5/5.0 Hz) was performed to observe the tumor appearance and to measure the maximum diameter of the nodule. The scan plane that allowed the most suitable depiction of the HCC lesion was carefully selected. Second, color Doppler ultrasound was used to evaluate the vascular abnormality within and around the tumor area. Third, contrast-enhanced ultrasound examinations were performed in harmonic imaging mode with a low mechanical index (0.21–0.30) chosen on the basis of a previous report [13]. The focal point was set at the deepest level of the HCC lesion. Gain was adjusted at an optimal level, and the dynamic range was set at 60–65 dB for unenhanced gray-scale ultrasound and 40–50 dB for contrast-enhanced ultrasound. These settings were used in all ultrasound examinations.

The perflubutane microbubble contrast agent (median bubble diameter, 2–3 μm) was administered to all patients at a dose of 0.0075 mL/kg by manual bolus injection followed by a flush of 5.0 mL normal saline solution through an antecubital or cubital vein. In cases of multiple hepatic lesions, the contrast agent was injected for observation of each lesion, and the additional injection was performed after the previous enhancement disappeared. After injection of the contrast agent, ultrasound images of the HCC lesion were obtained in the first minute by continuous scanning (15 Hz). Next, 5- and 10-minute phase images were obtained for a few seconds in each phase. Ultrasound examinations were conducted by three experts in hepatology and radiology (8, 8, and 20 years of experience in ultrasound examination). All images acquired were recorded digitally and reviewed at a later date by the observer with 20 years of experience, who was blinded to the clinical background of the patients. Contrast enhancement of HCC lesions was qualitatively assessed in each phase by comparison with enhancement of the adjacent liver parenchyma and classified as hyperenhancement, isoenhancement, or hypoenhancement.

Quantitative Assessment of Contrast-Enhanced Ultrasound Findings

Specialized software for intensity analysis (ImageLab, Toshiba) was used in this study (Fig. 1). First, a region of interest (ROI) was set manually on the whole HCC lesion on contrast-enhanced sonograms obtained during the first minute after contrast injection, and the time to reach the peak enhancement of the HCC lesion was measured on the time–intensity curve. Second, two ROIs the same size of the HCC lesion were set on the HCC lesion and adjacent liver parenchyma for calculation of the differences in intensity in the four phases: peak enhancement and 1, 5, and 10 minute after injection. Next, with an ROI the same size as the average diameter of the HCC lesion, the variability of contrast enhancement over the nontumor liver parenchyma was examined to obtain the reference value for assessment of contrast enhancement of the HCC lesion.

Three ROIs were set side by side on nontumor liver parenchyma at the same depth from the skin surface on the contrast-enhanced sonograms, and maximum differences in intensity among the three ROIs were calculated in the four phases. The average value of maximum intensity difference of nontumor liver parenchyma was calculated in each phase and defined as the intensity distribution in nontumor liver parenchyma. If the intensity difference between the HCC lesion and adjacent liver parenchyma was greater than the range of intensity distribution in nontumor liver parenchyma, the tumor finding was defined as hyperenhancement or hypoenhancement. If the intensity difference between the HCC lesion and adjacent liver parenchyma was within the range of the intensity distribution in nontumor liver parenchyma, the tumor finding was defined as isoenhancement. Washout in the HCC lesion was considered present when hyperenhancement or isoenhancement at peak enhancement shifted to hypoenhancement, and the presence or absence of washout was assessed in each phase.

One of the observers with 8 years of experience performed ROI positioning for the data used for the results. In addition, interobserver and intraobserver variability of intensity results for ROI positioning was examined with the ROI positioned by the other observer with 8 years of experience. Although we compared intensity-based and reading-based results, contrast enhancement of the tumor in this study was defined by the results of the intensity-based assessment.

CT During Hepatic Arteriography

CTHA was performed with an interventional radiology–CT system (Infinix Activ, Toshiba) after injection of 15 mL of iodinated contrast medium (iopamidol, Iopamiron 300, Bayer Schering Pharma) by mechanical power injector at a rate of 3 mL/s through a catheter placed in the common hepatic artery. For the arterial phase, images were obtained at 3 and 15 seconds after contrast administration. An expert in hepatology and radiology with 30 years of experience, who was blinded, evaluated the CTHA findings on the HCC lesions by comparing them with adjacent liver parenchyma and describing the appearance as hyperenhancement, isoenhancement, or hypoenhancement.

Statistical Analysis

All data are expressed as the mean ± SD or percentage. Statistically significant differences between contrast-enhanced ultrasound and CTHA with respect to detectability of tumor vascularity were examined by chi-square test. Agreement of contrast-enhanced ultrasound findings between intensity-based and reading-based assessment was examined with kappa statistics. A kappa value up to 0.2 indicated poor agreement; 0.2–0.4, slight agreement; 0.4 to 0.6, moderate agreement; 0.6

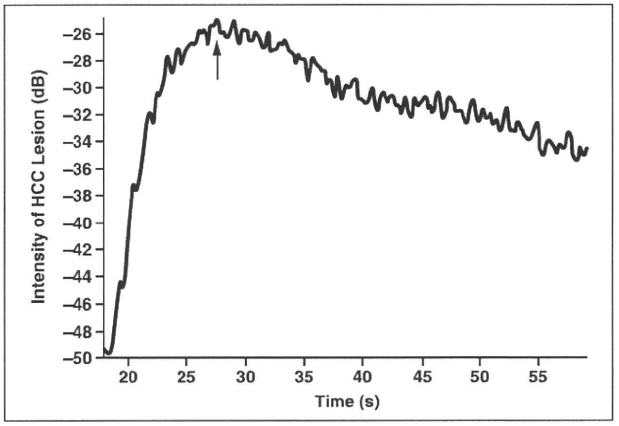

A

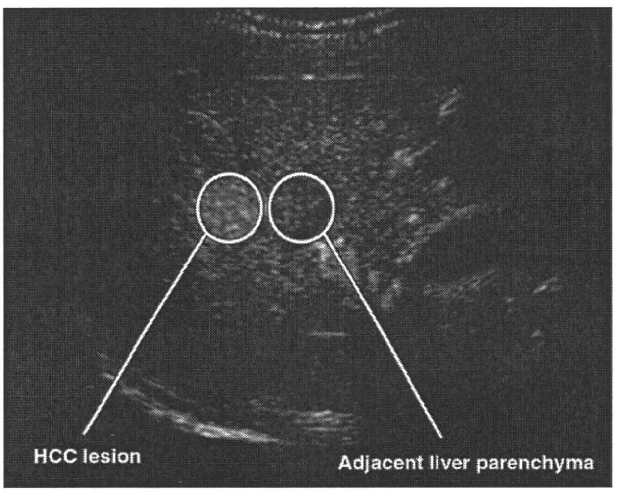

B

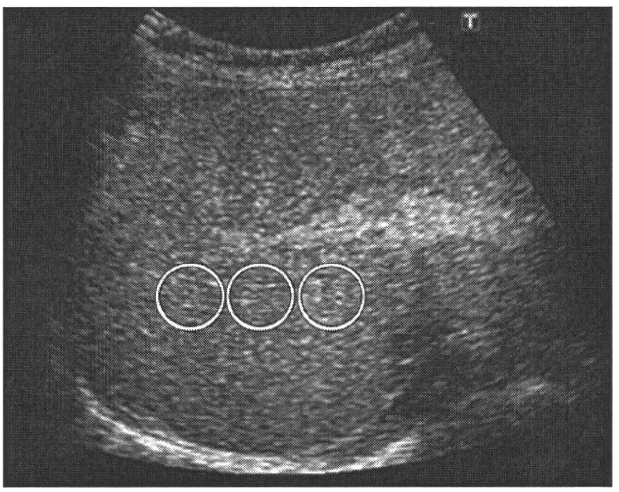

C

Fig. 1—Quantitative assessment of contrast-enhanced ultrasound findings of hepatocellular carcinoma (HCC).
A, Time–intensity curve for HCC lesion shows peak enhancement of nodule occurred 28 seconds (*arrow*) after contrast injection.
B, 64-year-old man with hepatitis C–related cirrhosis. Contrast-enhanced ultrasound image shows intensity-based quantitative assessment of contrast enhancement in HCC lesion. Two regions of interest (*circles*) were set at HCC lesion and adjacent liver parenchyma for calculation of difference in intensity between them.
C, Contrast-enhanced ultrasound image in same patient shows analysis of intensity distribution in nontumor liver parenchyma. Three regions of interest (*circles*) were set side by side in nontumor liver parenchyma at same depth from skin surface, and maximum difference in intensity among three regions of interest was calculated. In this way, average of maximum differences was calculated at peak enhancement and in 1-, 5-, and 10-minute phases as intensity distribution of nontumor liver parenchyma. If intensity difference between HCC lesion and adjacent liver parenchyma was greater than range of intensity distribution in nontumor liver parenchyma, tumor finding was defined as hyperenhancing or hypoenhancing. If intensity difference between HCC lesion and adjacent liver parenchyma was within range of intensity distribution in nontumor liver parenchyma, tumor finding was defined as isoenhancing.

to 0.8, good agreement; and greater than 0.8, excellent agreement. The relation between the frequency of washout after peak enhancement and cellular differentiation of HCC was examined by chi-square test followed by multiple comparison performed with the Ryan procedure. Interobserver and intraobserver variability of intensity results for positioning ROIs was examined with coefficient of variation (SD/mean × 100). The level of statistical significance was set at $p < 0.05$. Statistical analysis was performed with an SPSS software package (version 13.0 J, SPSS).

Results

Clinical Background

The 99 patients who met the inclusion criteria had 113 lesions; however, 27 lesions in 26 patients were excluded because the histologic diagnosis of 16 lesions was other than HCC (seven adenocarcinomas, nine benign nodules) and an insufficient amount of tissue was obtained from the other 11 lesions. In addition, nine lesions in nine patients that had a nodule-in-nodule CTHA appearance were excluded because two different pathologic components might have been present in the nodules. Therefore, we evaluated 77 HCC lesions (diameter, 19.1 ± 5.3 mm; range, 9.2–29.5 mm) in 64 patients (50 men, 14 women; mean age, 66.5 ± 9.6 years; range, 41–86 years). All 64 patients had cirrhosis. Four diagnoses of cirrhosis were based on the results of pathologic examination, and 60 were based on imaging findings, biochemical findings, and clinical symptoms. The cause of cirrhosis was hepatitis B virus infection in 13 patients, hepatitis C virus infection in 42 patients, alcohol abuse in five patients, autoimmune hepatitis in one patient, primary biliary cirrhosis in one patient, and cryptogenic processes in two patients.

The total number of HCC lesions was one in 52 patients, two in 11 patients, and three in one patient. The unenhanced gray-scale ultrasound pattern of 24 HCC lesions was hyperechoic, 10 lesions was isoechoic, 37 lesions was hypoechoic, and six lesions was heterogeneous. The histologic diagnosis of three HCC lesions was made with a surgical specimen and of 74 lesions was made after ultrasound-guided needle biopsy. Six HCC lesions were poorly differentiated; 45 lesions, moderately differentiated; and 26 lesions, well-differentiated. All the patients underwent surgery or biopsy within 2 weeks after contrast-enhanced ultrasound examination. The serum α-fetoprotein levels ranged from 1.8 to 1,266.1 ng/mL. The level was normal in 21 patients and abnormal in 43 patients (111.9 ± 240.0 ng/mL).

Contrast-Enhanced Ultrasound Findings at Peak Enhancement

The time–intensity analysis revealed that all HCC lesions exhibited peak enhancement within 1 minute after contrast injection. The

variability of contrast enhancement over the nontumor liver parenchyma in this phase was examined in 16 patients in whom three ROIs could be set side by side on nontumor liver parenchyma. The ultrasound plane of the liver in the other 48 patients did not have enough area for the three ROIs owing to the presence of relatively large intrahepatic vessels. Because the intensity distribution in nontumor liver parenchyma was 2.2 ± 0.6 dB, 64 lesions (83.1%) with an intensity difference of 10.0 ± 5.3 dB (range, 2.3–22.6 dB) between the lesions and adjacent liver parenchyma were classified as hyperenhancing. Similarly, 11 lesions (14.3%) with an intensity difference of 0.3 ± 1.2 dB (range, –2.0 to 1.9 dB) were classified as isoenhancing, and two lesions (2.6%) with an intensity difference of –5.9 ± 0.9 dB (range, –6.5 to –5.2 dB) were classified as hypoenhancing.

The interobserver and intraobserver variability of intensity results for ROI positioning was 4.7% and 3.1% for HCC lesions and 5.6% and 2.8% for nontumor hepatic parenchyma. Excellent agreement was found between intensity-based and reading-based assessment (κ = 0.912), although there were two cases of disagreement. One lesions was found to be isoenhancing according to reading-based assessment and hyperenhancing by intensity-based assessment. The other lesion was found isoenhancing by reading-based assessment and hypoenhancing by intensity-based assessment. Because CTHA showed hypervascularity in 63 of 77 lesions (81.8%), the concordance rate between contrast-enhanced ultrasound and CTHA with respect to hyperenhancement was 98.4% (63/64; Table 1 and Fig. 2). The detectability of tumor vascularity was not significantly different between these two modalities (p = 0.8553).

TABLE 1: Concordance Between Contrast-Enhanced Ultrasound and CT During Hepatic Arteriography With Respect to Enhancement of Hepatocellular Carcinoma (n = 77)

CT During Hepatic Arteriography	Contrast-Enhanced Ultrasound	
	Hyperenhancement	Isoenhancement or Hypoenhancement
Hyperenhancement	63	0
Isoenhancement or hypoenhancement	1	13

Note—p = 0.8553.

Washout Time After Peak Enhancement

In a procedure similar to that for the peak enhancement phase, the variability of contrast enhancement over the nontumor liver parenchyma 1, 5, and 10 minutes after contrast injection was examined in 16 patients. The findings were 1.6 ± 0.6 dB (range, 0.4–3.0 dB) in the 1-minute phase, 1.5 ± 0.4 dB (range, 0.8–2.2 dB) in the 5-minute phase, and 1.3 ± 0.5 dB (range, 0.3–2.0 dB) in the 10-minute phase. In total, 54 of the 64 lesions with hyperenhancement in the peak enhancement phase exhibited washout. In the 1-minute phase, 12 lesions exhibited an intensity difference of –5.9 ± 0.9 dB (range, –6.5 to –5.2 dB) between HCC lesions and adjacent liver parenchyma. In the 5-minute

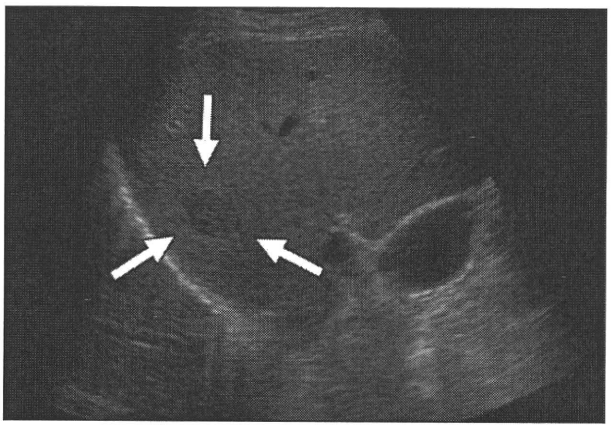

A

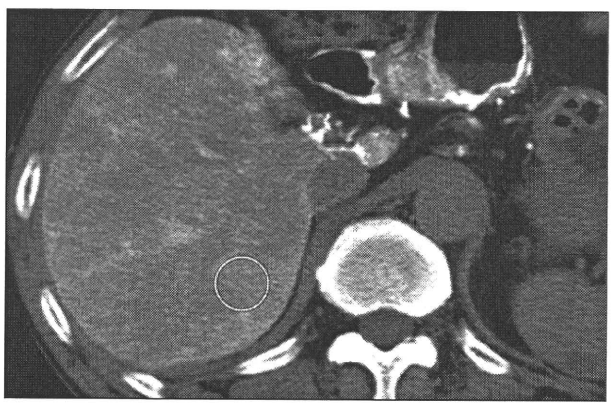

B

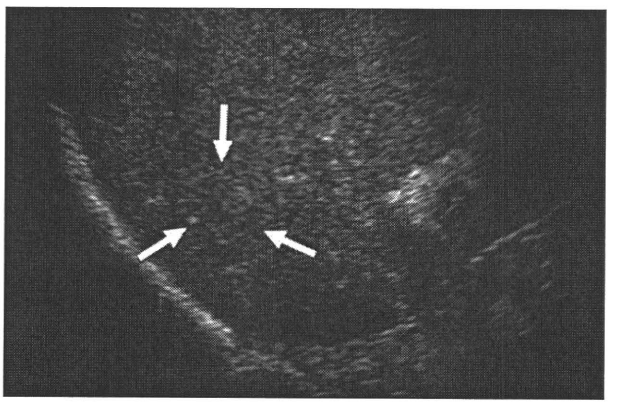

C

Fig. 2—72-year-old man with hepatitis C–related cirrhosis.
A, Unenhanced sonogram shows 17.0-mm-diameter hypoechoic lesion (*arrows*) in liver.
B, CT scan during hepatic arteriography obtained 15 seconds after contrast administration shows isoenhancing lesion (*circle*).
C, Contrast-enhanced sonogram at peak enhancement (35 seconds after agent injection) shows hyperenhancement (*arrows*) in lesion, which was diagnosed as moderately differentiated hepatocellular carcinoma after ultrasound-guided needle biopsy.

TABLE 2: Relation Between Cellular Differentiation of Hyperenhancing Hepatocellular Carcinoma at Peak Enhancement (n = 64) and Phase at Which Washout Occurred

Differentiation	1-Minute Phase	5-Minute Phase	10-Minute Phase
Poor (n = 6)	4 (66.7)[a,b]	6 (100)	6 (100)
Moderate (n = 42)	8 (19.0)[a]	35 (83.3)[c]	38 (90.5)[d]
Well (n = 16)	0 (0)[b]	7 (43.8)[c]	10 (62.5)[d]

Note—Values are number of hepatocellular carcinoma lesions with percentages in parentheses.
[a] $p = 0.0117$.
[b] $p = 0.0003$.
[c] $p = 0.0026$.
[d] $p = 0.0117$.

phase, 48 lesions exhibited an intensity difference of –4.4 ± 1.7 dB (range, –7.3 to –1.9 dB). In the 10-minute phase, 54 lesions exhibited an intensity difference of –5.3 ± 2.4 dB (range, –16.2 to –1.9 dB). The other 10 lesions, which had an intensity difference of –0.6 ± 0.6 dB (range, –1.0 to 0.5 dB), were classified as isoenhancing in the 10-minute phase. The 13 lesions that were isoenhancing or hypoenhancing at peak enhancement had an intensity difference of –0.3 ± 0.7 dB (range, –1.2 to 0.8 dB) in the 10-minute phase. Therefore, these 23 lesions did not exhibit washout during enhancement.

The contrast-enhanced ultrasound findings obtained at intensity-based and reading-based assessment exhibited excellent agreement in all three phases after peak enhancement: kappa values of 0.847 for the 1-minute phase, 0.915 for the 5-minute phase, and 0.970 for the 10-minute phase. All seven cases of disagreement about the 1-, 5-, and 10-minute phase images were lesions that were isoenhancing by reading-based assessment and hypoenhancing by intensity-based assessment. The interobserver and intraobserver variability of intensity results for positioning ROIs was calculated in each phase. The results were 6.2% and 4.0% for HCC lesions and 5.6% and 4.7% for nontumor liver parenchyma in the 1-minute phase, 8.0% and 5.8% for HCC lesions and 7.4% and 3.4% for nontumor liver parenchyma in the 5-minute phase, and 7.4% and 5.7% for HCC lesions and 7.9% and 5.6% for nontumor liver parenchyma in the 10-minute phase.

Relation Between Contrast-Enhanced Ultrasound Findings on HCC Lesions and Cellular Differentiation

Among 64 lesions hyperenhancing at peak enhancement, four poorly differentiated HCCs and eight moderately differentiated HCCs exhibited washout within 1 minute after contrast administration (Table 2 and Fig. 3). Thirty-six lesions in addition to these 12 exhibited washout in the 5-minute phase: six poorly differentiated, 35 moderately differentiated, and seven well-differentiated HCCs, for a total of 48 lesions exhibiting washout in the 5-minute phase (Fig. 4). Similarly, because six lesions that did not exhibit washout in the 5-minute phase appeared as washout in the 10-minute

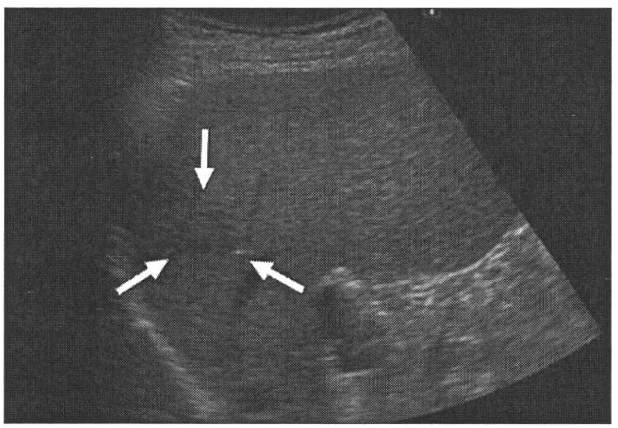

A

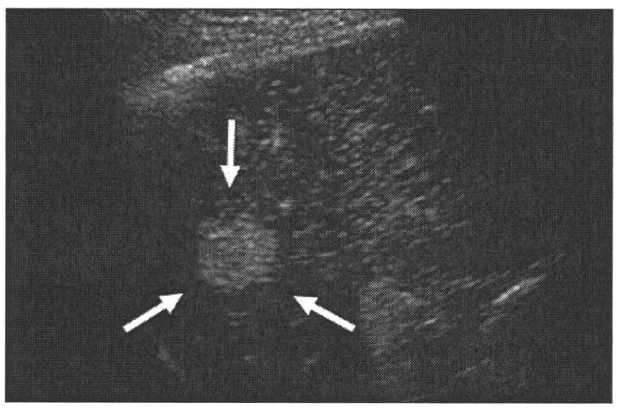

B

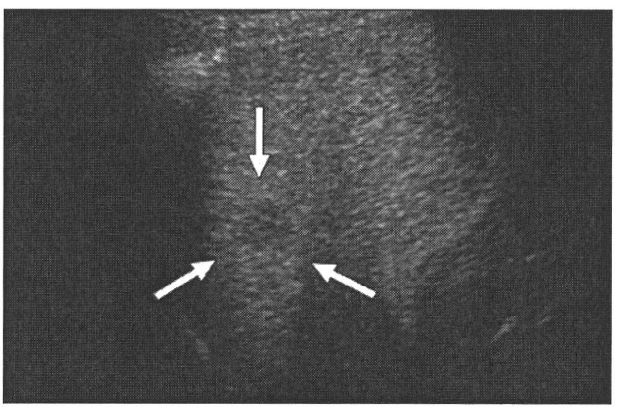

C

Fig. 3—62-year-old man with hepatitis B–related cirrhosis.
A, Unenhanced sonogram shows hypoechoic 17.1-mm-diameter lesion (*arrows*) in liver.
B, Contrast-enhanced sonogram at peak enhancement (31 seconds after injection) shows hyperenhancing lesion (*arrows*).
C, Contrast-enhanced sonogram obtained in 1-minute phase (56 seconds after agent injection) shows hypoenhancing lesion (*arrows*), which was diagnosed as poorly differentiated hepatocellular carcinoma after ultrasound-guided needle biopsy.

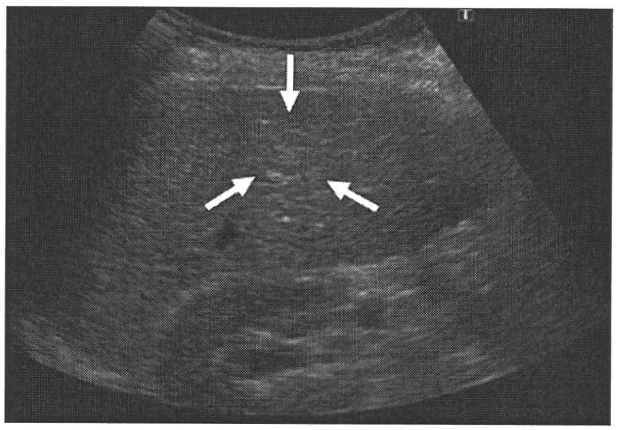

A

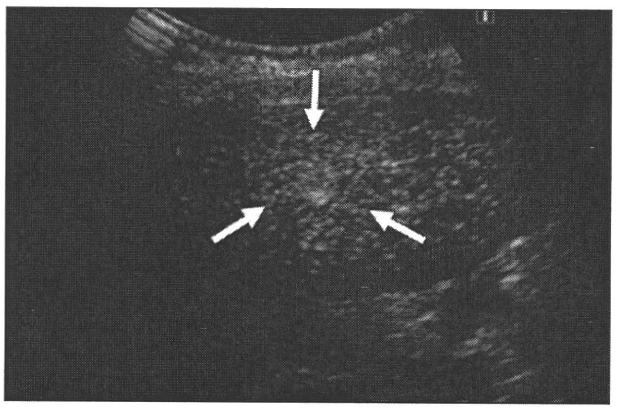

B

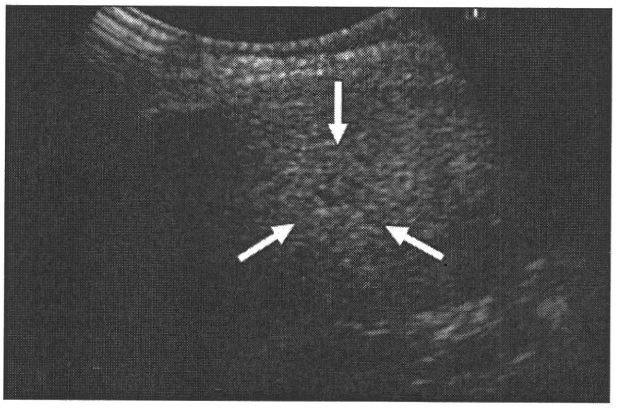

C

Fig. 4—69-year-old woman with hepatitis C–related cirrhosis.
A, Unenhanced sonogram shows 12.3-mm-diameter isoechoic lesion (*arrows*) in liver.
B, Contrast-enhanced sonogram at peak enhancement (28 seconds after injection) shows hyperenhancing lesion (*arrows*).
C, Contrast-enhanced sonogram obtained in 5-minute phase (5 minutes 4 seconds after injection) shows hypoenhancing lesion (*arrows*), which was diagnosed as moderately differentiated hepatocellular carcinoma after ultrasound-guided needle biopsy.

phase, a total of 54 lesions exhibited washout in this final phase: six poorly differentiated HCCs, 38 moderately differentiated, and 10 well-differentiated HCCs. Washout was significantly more frequent for poorly differentiated HCC than for moderately differentiated HCC ($p = 0.0117$) or well-differentiated HCC ($p = 0.0003$) in the 1-minute phase and more frequent for moderately differentiated than for well-differentiated HCC in the 5-minute phase ($p = 0.0026$) and the 10-minute phase ($p = 0.0117$). The 10 lesions without washout in the 10-minute phase (four moderately differentiated and six well-differentiated HCCs) were isoenhancing (Fig. 5). Although three of the 11 lesions with isoenhancement at peak enhancement were moderately differentiated HCC, the other eight isoenhancing lesions and two hypoenhancing lesions were well-differentiated HCC.

Discussion

Step-by-step differentiation is the estimated natural progression of HCC [19, 20, 22, 23], and the changes in tumor appearance can be appreciated at imaging. As shown in our results, only poorly and moderately differentiated HCC exhibited washout within 1 minute, but the appearance was found predominantly in poorly differentiated HCC (66.7%). Cellular differentiation is a significant factor in prognosis and recurrence among HCC patients after liver transplant, and fine-needle biopsy of the tumor is recommended for pretransplant workup [24]. In addition, because the risk of metastasis increases in cases of poorly differentiated HCC, evaluation of cellular differentiation affects patient care [25]. Noninvasive prediction of differentiation with perflubutane microbubble–enhanced sonography should have considerable benefit in the clinical management of HCC.

The sonographic shift of a hepatic tumor from hyperenhancement to hypoenhancement according to imaging phase is a well-known phenomenon in contrast-enhanced ultrasound [12, 14, 26]. There are several explanations for the relation between cellular differentiation and washout timing of perflubutane microbubble–related contrast enhancement. First, the presence of Kupffer cells in the HCC lesion may account for the shift of washout timing. Studies have shown a relation between distribution of Kupffer cells in the HCC lesion and its cellular differentiation [27–29], and phagocytosis by Kupffer cells is one of the proposed mechanisms for accumulation of perflubutane microbubbles in the liver [16, 17]. It remains to be elucidated, however, when accumulation of the microbubbles starts after the agent is injected and whether accumulated microbubbles play a role as a signal enhancer. Second, structural differences in the blood sinus in HCC lesions related to cellular differentiation may explain the difference in washout timing. That is, the greater the structural difference between sinusoids in adjacent liver parenchyma and the blood sinus in HCC becomes, the faster the passage of microbubbles in HCC. Results of some studies support this hypothesis. Using perflutren lipid microspheres (Definity, Lantheus Medical Imaging), a blood pool contrast

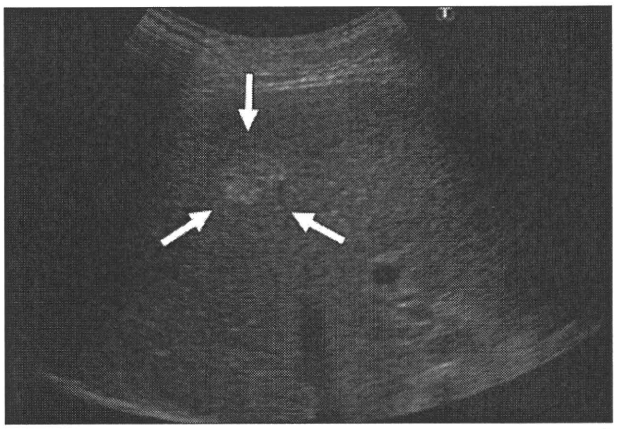

A

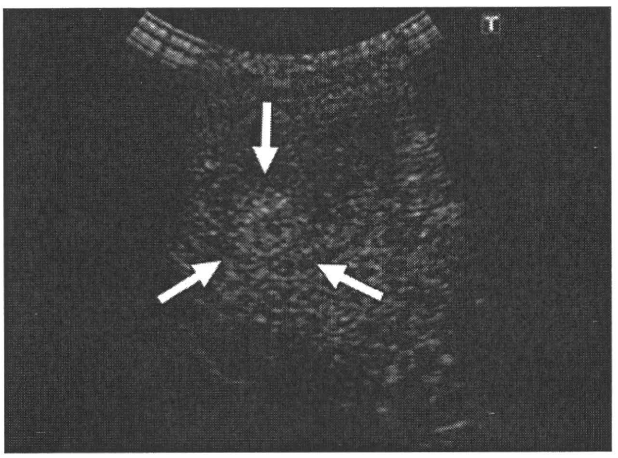

B

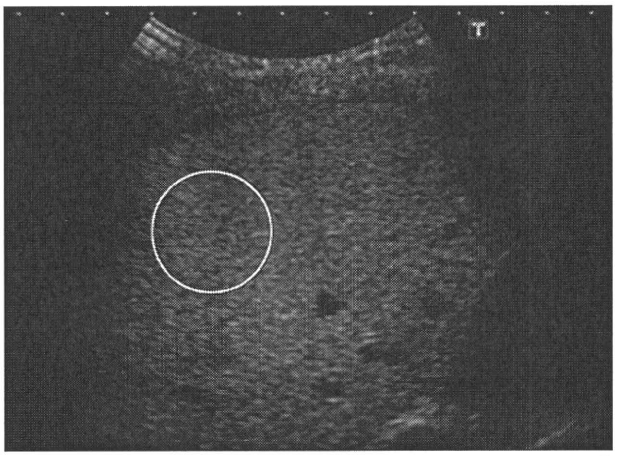

C

Fig. 5—78-year-old man with hepatitis C–related cirrhosis.
A, Unenhanced sonogram shows 17.9-mm-diameter hyperechoic lesion (*arrows*) in liver.
B, Contrast-enhanced sonogram at peak enhancement (45 seconds after injection) shows hyperenhancing lesion (*arrows*).
C, Contrast-enhanced sonogram obtained in 10-minute phase (10 minutes 10 seconds after injection) shows isoenhancing lesion (*circle*), which was diagnosed as well-differentiated hepatocellular carcinoma after ultrasound-guided needle biopsy.

agent that does not accumulate in the liver. Jang et al. [30] found that earlier shift of washout time in HCC was related to tumor differentiation. They mentioned that total lack of similarity to the normal hepatocyte and its architecture in poorly differentiated HCC may be the explanation for the earliest washout time in the lesion. Nicolau et al. [31] reported that hypoenhancement with an aqueous suspension of phospholipid-stabilized microbubbles filled with sulfur hexafluoride (SonoVue, Bracco), which also is a blood pool contrast agent, was more frequent after the arterial phase of enhancement as differentiation of HCC progressed. Another study with aqueous suspension of phospholipid-stabilized microbubbles filled with sulfur hexafluoride also showed that hypovascularity in the portal venous phase was more frequent in moderately and poorly differentiated HCC than in well-differentiated HCC [32]. These results suggest that the earlier shift of washout time may be common in contrast-enhanced ultrasound regardless of the type of agent, that is, with or without accumulation activity in the liver, although a continuous study may be necessary to prove this point.

Another aspect of washout in contrast-enhanced ultrasound is strong suspicion of a malignant lesion, whereas isoenhancement in the delayed phase seems to suggest a lesion is benign [14]. It has been reported [32] that differentiation between benign and malignant nodules measuring 2 cm or smaller that are hypervascular in the arterial phase and isovascular or hypervascular in the portal venous phase cannot be achieved with contrast-enhanced ultrasound because such findings are seen in both well-differentiated HCC and hypervascular benign nodules. Although our study did not include benign hepatic lesions, we emphasize that isoenhancement in the late phase does not always feature a benign lesion. In our study, 9.5% of moderately differentiated HCCs and 37.5% of well-differentiated HCCs exhibited late phase isoenhancement. Characterization of hepatic lesions without hypoenhancement after peak enhancement should be a future challenge.

The concordance rate between contrast-enhanced ultrasound and CTHA with respect to hyperenhancement was 98.4% (63/64). Discrepancy occurred in only one case: hyperenhancement at contrast-enhanced ultrasound and isoenhancement at CTHA. Because it is believed that CTHA yields the highest rate of detection of tumor vascularity [33, 34], there is no standard imaging tool other than CTHA for judging contrast-enhanced ultrasound findings, and false-positive results of ultrasound cannot be denied. However, we emphasize that the rate of detection of tumor vascularity with contrast-enhanced ultrasound with the perflubutane microbubble agent was at least the same as that with CTHA. As previously discussed, CTHA requires an invasive procedure and

excessive radiation exposure [35]. Despite its operator- and patient-dependent nature, contrast-enhanced ultrasound with the perflubutane microbubble agent can be expected to be a standard method for assessment of tumor vascularity.

It has been reported [30] that there was no significant difference between the washout time of hypervascular HCC in noncirrhotic liver and that in severely fibrotic liver, although the differentiation of HCC in each group was not provided in the report. We speculated, however, that depending on the hemodynamics of the hepatic artery and portal vein and microbubble accumulation by the reticuloendothelial system, time-related changes in the contrast enhancement of HCC lesions may be affected by enhancement of adjacent hepatic parenchyma. Although all of the subjects in our study had cirrhosis, parenchymal enhancement itself might vary according to the severity of liver damage. We therefore based quantitative assessment of tumor enhancement on the intensity distribution in the nontumor area to minimize the effect of parenchymal enhancement. Objective assessment of contrast enhancement between HCC lesions and adjacent liver parenchyma showed excellent agreement with the results of subjective assessment in our study, although there were a few cases of disagreement in every phase. In addition, the results of intensity measurement showed sufficient interobserver and intraobserver variability for positioning ROIs, representing reliable procedure. However, because analysis of intensity can be complicated, an automatic measurement process should be introduced for assessment of the contrast-enhanced ultrasound findings.

There were shortcomings to our study. The first was that hepatic tumors comprised only HCC, not other tumors, such as cholangiocellular carcinoma, hypervascular metastatic liver cancer, hemangioma, and focal nodular hyperplasia. Because differential diagnosis between HCC and these liver tumors sometimes is required, time-related changes in contrast enhancement should be examined for these hepatic lesions. The second limitation was that our study included a small number of hypovascular and isovascular HCCs and no borderline lesions such as dysplastic nodules. Because most of the pathologic specimens were obtained by percutaneous needle biopsy with a 21-gauge needle, we cannot deny the difficulty of differentiation between dysplastic nodule and well-differentiated HCC; some high-grade dysplastic nodules might have been classified as well-differentiated HCC. The third limitation was that we observed contrast enhancement only up to 10 minutes after contrast injection. Although observation for more than 10 minutes may not be practical, a previous report [21] showed the usefulness of contrast enhancement 30 minutes after injection in the assessment of cellular differentiation of HCC. The appropriate time for observation of contrast enhancement according to specific purpose should be established in the near future.

We conclude that the washout time of perflubutane microbubble–related contrast enhancement in HCC lesions was closely related to cellular differentiation of HCC. Although further studies involving a large patient sample may be necessary to confirm the results, we believe our technique has potential for obviating needle biopsy in the assessment of cellular differentiation of HCC.

References

1. Llovet JM, Burroughs A, Bruix J. Hepatocellular carcinoma. *Lancet* 2003; 362:1907–1917
2. Bruix J, Llovet JM. Prognostic prediction and treatment strategy in hepatocellular carcinoma. *Hepatology* 2002; 35:519–524
3. Carr BI. Hepatocellular carcinoma: current management and future trends. *Gastroenterology* 2004; 127:S218–S224
4. Asayama Y, Yoshimitsu K, Nishihara Y, et al. Arterial blood supply of hepatocellular carcinoma and histologic grading: radiologic-pathologic correlation. *AJR* 2008; 190:90; [web]W28–W34
5. Bruix J, Sherman M, Llovet JM, et al. Clinical management of hepatocellular carcinoma; conclusions of the Barcelona-2000 EASL conference. European Association for the Study of the Liver. *J Hepatol* 2001; 35:421–430
6. Murakami T, Kim T, Takamura M, et al. Hypervascular hepatocellular carcinoma: detection with double arterial phase multi-detector row helical CT. *Radiology* 2001; 218:763–767
7. Bolondi L, Gaiani S, Celli N, et al. Characterization of small nodules in cirrhosis by assessment of vascularity: the problem of hypovascular hepatocellular carcinoma. *Hepatology* 2005; 42:27–34
8. Roncalli M, Roz E, Coggi G, et al. The vascular profile of regenerative and dysplastic nodules of the cirrhotic liver: implications for diagnosis and classification. *Hepatology* 1999; 30:1174–1178
9. Matsui O, Kadoya M, Kameyama T, et al. Benign and malignant nodules in cirrhotic livers: distinction based on blood supply. *Radiology* 1991; 178:493–497
10. Takayasu K, Muramatsu Y, Furukawa H, et al. Early hepatocellular carcinoma: appearance at CT during arterial portography and CT arteriography with pathologic correlation. *Radiology* 1995; 194:101–105
11. Giorgio A, Ferraioli G, Tarantino L, et al. Contrast-enhanced sonographic appearance of hepatocellular carcinoma in patients with cirrhosis: comparison with contrast-enhanced helical CT appearance. *AJR* 2004; 183:1319–1326
12. Lencioni R; European Federation of Societies for Ultrasound in Medicine and Biology (EFSUMB). Impact of European Federation of Societies for Ultrasound in Medicine and Biology (EFSUMB) guidelines on the use of contrast agents in liver ultrasound. *Eur Radiol* 2006; 16:1610–1613
13. Maruyama H, Takahashi M, Ishibashi H, et al. Ultrasound-guided treatments under low acoustic power contrast harmonic imaging for hepatocellular carcinomas undetected by B-mode ultrasonography. *Liver Int* 2009; 29:708–714
14. Quaia E, Calliada F, Bertolotto M, et al. Characterization of focal liver lesions with contrast-specific US modes and a sulfur hexafluoride-filled microbubble contrast agent: diagnostic performance and confidence. *Radiology* 2004; 232:420–430
15. Wilson SR, Burns PN, Muradali D, Wilson JA, Lai X. Harmonic hepatic US with microbubble contrast agent: initial experience showing improved characterization of hemangioma, hepatocellular carcinoma, and metastasis. *Radiology* 2000; 215:153–161
16. Watanabe R, Matsumura M, Chen CJ, Kaneda Y, Fujimaki M. Characterization of tumor imaging with microbubble-based ultrasound contrast agent, Sonazoid, in rabbit liver. *Biol Pharm Bull* 2005; 28:972–977
17. Marelli C. Preliminary experience with NC100100, a new ultrasound contrast agent for intravenous injection. *Eur Radiol* 1999; 9[suppl 3]:S343–S346
18. Kojiro M. Focus on dysplastic nodules and early hepatocellular carcinoma: an Eastern point of view. *Liver Transpl* 2004; 10:S3–S8
19. Sakamoto M, Hirohashi S, Shimosato Y. Early stages of multistep hepatocarcinogenesis: adenomatous hyperplasia and early hepatocellular carcinoma. *Hum Pathol* 1991; 22:172–178
20. Takayama T, Makuuchi M, Hirohashi S, et al. Malignant transformation of adenomatous hyperplasia to hepatocellular carcinoma. *Lancet* 1990; 336:1150–1153
21. Korenaga K, Korenaga M, Furukawa M, Yamasaki T, Sakaida I. Usefulness of Sonazoid contrast-enhanced ultrasonography for hepatocellular carcinoma: comparison with pathological diagnosis and superparamagnetic iron oxide magnetic resonance images. *J Gastroenterol* 2009; 44:733–741

22. Kojiro M, Nakashima O. Histopathologic evaluation of hepatocellular carcinoma with special reference to small early stage tumors. *Semin Liver Dis* 1999; 19:287–296
23. Oikawa T, Ojima H, Yamasaki S, Takayama T, Hirohashi S, Sakamoto M. Multistep and multicentric development of hepatocellular carcinoma: histological analysis of 980 resected nodules. *J Hepatol* 2005; 42:225–229
24. Zavaglia C, De Carlis L, Alberti AB, et al. Predictors of long-term survival after liver transplantation for hepatocellular carcinoma. *Am J Gastroenterol* 2005; 100:2708–2716
25. Si MS, Amersi F, Golish SR, et al. Prevalence of metastases in hepatocellular carcinoma: risk factors and impact on survival. *Am Surg* 2003; 69:879–885
26. Gaiani S, Celli N, Piscaglia F, et al. Usefulness of contrast-enhanced perfusional sonography in the assessment of hepatocellular carcinoma hypervascular at spiral computed tomography. *J Hepatol* 2004; 41:421–426
27. Imai Y, Murakami T, Yoshida S, et al. Superparamagnetic iron oxide-enhanced magnetic resonance images of hepatocellular carcinoma: correlation with histological grading. *Hepatology* 2000; 32:205–212
28. Inoue T, Kudo M, Watai R, et al. Differential diagnosis of nodular lesions in cirrhotic liver by post-vascular phase contrast-enhanced US with Levovist: comparison with superparamagnetic iron oxide magnetic resonance images. *J Gastroenterol* 2005; 40:1139–1147
29. Tanaka M, Nakashima O, Wada Y, Kage M, Kojiro M. Pathomorphological study of Kupffer cells in hepatocellular carcinoma and hyperplastic nodular lesions in the liver. *Hepatology* 1996; 24:807–812
30. Jang HJ, Kim TK, Burns PN, Wilson SR. Enhancement patterns of hepatocellular carcinoma at contrast-enhanced US: comparison with histologic differentiation. *Radiology* 2007; 244:898–906
31. Nicolau C, Catala V, Vilana R, et al. Evaluation of hepatocellular carcinoma using SonoVue, a second generation ultrasound contrast agent: correlation with cellular differentiation. *Eur Radiol* 2004; 14:1092–1099
32. Quaia E, D'Onofrio M, Cabassa P, et al. Diagnostic value of hepatocellular nodule vascularity after microbubble injection for characterizing malignancy in patients with cirrhosis. *AJR* 2007; 189:1474–1483
33. Irie T, Takeshita K, Wada Y, et al. CT evaluation of hepatic tumors: comparison of CT with arterial portography, CT with infusion hepatic arteriography, and simultaneous use of both techniques. *AJR* 1995; 164:1407–1412
34. Kanematsu M, Hoshi H, Murakami T, et al. Detection of hepatocellular carcinoma in patients with cirrhosis: MR imaging versus angiographically assisted helical CT. *AJR* 1997; 169:1507–1515
35. Chezmar JL, Bernardino ME, Kaufman SH, Nelson RC. Combined CT arterial portography and CT hepatic angiography for evaluation of the hepatic resection candidate: work in progress. *Radiology* 1993; 189:407–410

ALCOHOLISM: CLINICAL AND EXPERIMENTAL RESEARCH

Vol. 35, No. 2
February 2011

Increased Serum Levels of Pigment Epithelium-Derived Factor by Excessive Alcohol Consumption—Detection and Identification by a Three-Step Serum Proteome Analysis

Kazuyuki Sogawa, Yoshio Kodera, Mamoru Satoh, Yusuke Kawashima, Hiroshi Umemura, Katsuya Maruyama, Hirotaka Takizawa, Osamu Yokosuka, and Fumio Nomura

Background: The search for biological markers of alcohol abuse is of continual interest in experimental and clinical alcohol research. We previously used gel-free proteome analysis methods such as the ProteinChip® system and the ClinProt™ system to search for new serum markers for alcoholism and found several novel marker candidates. As serum contains thousands of proteins and peptides that are present in a large dynamic concentration, depletion of the abundant proteins and further fractionation of the remainder is necessary to get into the deep proteome. We recently described a simple and highly reproducible three-step method for identifying potential disease-marker candidates among the low-abundance serum proteins.

Methods: Two serum samples—one on admission and one after 8 weeks of abstinence—were obtained from 8 patients with alcohol dependency. The samples were subjected to a three-step serum proteome analysis. The steps were the following: first, immunodepletion of the 6 most abundant proteins; second, fractionation using reverse-phase high-performance liquid chromatography; and third, separation using one-dimensional sodium dodecyl sulfate polyacrylamide gel electrophoresis (SDS–PAGE). Differences revealed by protein staining were further confirmed by Western blotting and by enzyme-linked immunosorbent assays (ELISA).

Results: Three-step serum proteome analysis revealed that the serum levels of 5 proteins, alpha2-HS glycoprotein, apolipoprotein A-I, glutathione peroxidase 3, heparin cofactor II, and pigment epithelial-derived factor (PEDF), were significantly greater on admission than after 8 weeks of abstinence. We focused on PEDF because alterations in its levels in alcoholic subjects are not well known. Western blotting and ELISA confirmed the upregulation of PEDF. Serum PEDF levels were significantly greater in moderate to heavy habitual drinkers (14.2 ± 7.7 μg/ml) than in healthy subjects without a drinking history (5.5 ± 3.0 μg/ml) ($p < 0.001$). The serum PEDF levels in subjects with nonalcoholic chronic liver diseases were comparable to the PEDF levels in healthy subjects.

Conclusion: Three-step serum proteome analysis reveals that excessive alcohol drinking increases the PEDF level.

Key Words: Alcoholism, Pigment Epithelial-Derived Factor, Proteomics, Serum.

EXCESSIVE ALCOHOL CONSUMPTION causes alcoholism and alcoholic liver diseases and aggravates many common medical problems such as hypertension, diabetes mellitus, and gout. Although the primary strategy for detecting heavy drinking relies on self-reporting, heavy drinkers tend to underestimate their alcohol consumption. This leads to an underdiagnosis of hazardous alcohol use and related disorders (Alling et al., 2005). Therefore, the search for biological markers of alcohol abuse is of continual interest in experimental and clinical alcohol research (Hannuksela et al., 2007; Niemela, 2007; Nomura et al., 2007).

We previously used the ProteinChip® system to search for new serum markers of alcoholism and found several novel marker candidates (Nomura et al., 2004). Of these markers, a 5.9-kDa peptide (which is a fragment of the fibrinogen alpha chain) with an *m/z* of 5890 was useful in detecting gamma-glutamyltransferase (GGT) nonresponders in male subjects seeking a medical checkup (Sogawa et al., 2007). More recently, we used the ClinProt™ system (Bruker Daltonics, Bremen, Germany; consisting of a combination of beads processing and matrix-assisted laser desorption/ionization

From the Clinical Proteomics Research Center (KS, YK, MS, YK, FN), Chiba University Hospital, Chiba, Japan; Department of Physics (YK), School of Science, Kitasato University, Kanagawa, Japan; Department of Molecular Diagnosis (HU, FN), Graduate School of Medicine, Chiba University, Chiba, Japan; National Hospital Organization Kurihama Alcoholism Center (KM), Kanagawa, Japan; Kashiwado Clinic in Port-Square (HT), Kashiwado Memorial Foundation, Chiba, Japan; and Division of Gastroenterology (OY), Chiba University Hospital, Chiba, Japan.

Received for publication April 26, 2010; accepted July 18, 2010.

Reprint requests: Fumio Nomura, MD, PhD, Department of Molecular Diagnosis, Graduate School of Medicine, Chiba University, 1-8-1 Inohana, Chuo-ku, Chiba City, Chiba 260-8670, Japan; Fax: +81-43-226-2324; E-mail: fnomura@faculty.chiba-u.jp

DOI: 10.1111/j.1530-0277.2010.01336.x

time-of-flight mass spectroscopy [MALDI-TOF MS]) to facilitate close analysis of serum peptide markers not detectable by the ProteinChip® system. We found 4 other peaks as candidate peptide markers (Sogawa et al., 2009).

A technical challenge in serum proteome analysis is that serum contains thousands of proteins and peptides that are present in a large dynamic concentration. Indeed, 22 abundant proteins such as albumin, immunoglobulins, and transferrin constitute up to 99% of the protein content of plasma (Anderson and Anderson, 2002; Tirumalai et al., 2003). Depletion of these abundant proteins and further fractionation of samples will be necessary in future proteomic studies searching for low-abundance serum proteins or peptides.

We recently described a simple and highly reproducible three-step method for identifying potential disease-marker candidates among the low-abundance serum proteins (Kawashima et al., 2009). Using this method, we successfully identified 3 proteins, including YKL-50, as promising biomarkers of sepsis (Hattori et al., 2009). The three steps are the following: first, immunodepletion of the abundant proteins; second, fractionation using reverse-phase high-performance liquid chromatography (HPLC); and third, one-dimensional sodium dodecyl sulfate polyacrylamide gel electrophoresis (SDS–PAGE). In this study, we applied this three-step proteome analysis method to gain more insight into the alterations of serum proteins resulting from excessive alcohol consumption. We detected and identified increased pigment epithelial-derived factor (PEDF) serum levels after excessive alcohol consumption.

MATERIALS AND METHODS

Patients

Sequential serum samples were obtained from patients with alcohol dependency on admission and after 8 weeks of abstinence. The patients were diagnosed in accordance with the DSM IV criteria (American Psychiatric Association, 1994) and admitted to the National Hospital Organization Kurihama Alcoholism Center (Kanagawa, Japan). All of the patients consumed more than 100 g of alcohol per day for more than 10 years until the day of hospitalization.

A total of 120 patients with biopsy-proven nonalcoholic liver diseases were included. In this group, 20 patients had chronic hepatitis B; 20 patients had liver cirrhosis because of hepatitis B virus (HBV) infection; 20 patients had chronic hepatitis C; 20 patients had liver cirrhosis because of hepatitis C virus (HCV) infection; 20 patients had autoimmune hepatitis; and 20 patients had primary biliary cirrhosis.

Blood samples were also obtained from 60 apparently healthy subjects with various drinking habits who visited the Kashiwado Clinic in Port-Square of Kashiwado Memorial Foundation (Chiba, Japan) for their annual medical checkup. All subjects were administered a detailed questionnaire concerning the amount of alcoholic beverages consumed (calculated as grams of ethanol per day), the duration of drinking, and the frequency of drinking. Twenty nondrinkers, 20 light drinkers (less than 40 g/d), and 20 heavy drinkers (more than 80 g/d) were randomly selected from subjects who sought a medical checkup. These subgroups were defined by the criteria reported by Conigrave and colleagues (2002).

The demographic data of the subjects studied are presented in Table 1.

All the serum samples were collected, processed in a protocol that we previously described (Umemura et al., 2009), and stored at −80°C in aliquots until analysis. All of the subjects provided written informed consent, and the Ethics Committee of Chiba University School of Medicine approved this study.

The Removal of High-Abundance Proteins From the Serum Samples

The first step of the three-step analysis involved removing the 6 major serum proteins—albumin, immunoglobulin G, alpha-1-antitrypsin, immunoglobulin A, transferrin, and haptoglobin—by passing them through a commercially available immunoaffinity column, the Multi Affinity Removal column (Agilent Technologies Inc., Santa Clara, CA). Twenty-five microliters of serum was diluted to 75 μL with a loading buffer (Agilent Technologies Inc.) and spin-filtered (0.22 μm) for 30 min at 13,000 rpm and 4°C. One hundred microliters of each sample was injected from an autosampler cooled to 4°C. Depletion was performed at room temperature on a Shimadzu LC10A VP HPLC system (Shimadzu Co., Kyoto, Japan), using the following program: 9 min at 100% eluent A (Agilent Technologies Inc.) at 0.25 ml/min; 3.5 min at 100% eluent B (Agilent Technologies Inc.) at 1.0 ml/min; and then 7.5 min at 100% eluent A at 1.0 ml/min. Based on the chromatogram, which was recorded by measuring the absorbance of the eluate at 280 nm, the flow-through fractions eluted at a retention time between 2.5 min and 6.5 min were collected in eight 0.125 mL aliquots (for a total volume of 1.0 ml). Using Vivaspin 2 Polyethersulfone spin concentrators (molecular weight cutoff at 10 kDa; Vivascience, Hannover, Germany), the flow-through fractions were combined and concentrated by centrifugal ultrafiltration to a total volume of 80 μL. The concentrated sample solution was stored at −80°C until use.

Table 1. Demographic Data of Subjects Studied

Experimental diseases (number of patients)	Sex (M/F)	Age (mean ± SD)	Alcohol consumption (mean ± SD g/d)
Alcohol dependency (n = 20)	20/0	52.8 ± 11.9	201.3 ± 57.3
Healthy volunteers			
Nondrinkers (n = 20)	20/0	50.9 ± 9.0	–
Low-risk drinkers (n = 20)	20/0	50.0 ± 5.3	30.0 ± 6.2
High-risk drinkers (n = 20)	20/0	50.4 ± 6.5	107.5 ± 35.2
Nonalcoholic liver disease			
Hepatitis B virus infection			
Chronic hepatitis (n = 20)	10/10	49.2 ± 14.6	–
Liver cirrhosis (n = 20)	10/10	61.6 ± 9.3	–
Hepatitis C virus infection			
Chronic hepatitis (n = 20)	12/8	63.9 ± 14.6	–
Liver cirrhosis (n = 20)	12/8	69.4 ± 8.5	–
Autoimmune hepatitis (n = 20)	4/16	61.7 ± 15.3	–
Primary biliary cirrhosis (n = 20)	4/16	63.2 ± 8.3	–

Reverse-Phase High-Performance Liquid Chromatography

The second step of the three-step analysis involved subjecting the concentrated flow-through fractions (75 μL) to the Intrada WP-RP column (Imtakt, Kyoto, Japan), which was attached to an HPLC system (NANOSPACE SI-2 system; Shiseido Fine Chemicals, Tokyo, Japan). We conducted chromatography, as previously described (Kawashima et al., 2009). Each fraction was dried in a centrifugal vacuum concentrator and stored at −80°C for subsequent SDS–PAGE analysis.

SDS–PAGE Analysis

The third step of the three-step analysis involved subjecting each HPLC fraction to SDS–PAGE. The lyophilized samples of the HPLC fractions were dissolved in a PAGE sample buffer (pH 6.8; 50 mM Tris–HCl, 50 mM dithiothreitol, 0.5% SDS and 10% glycerol). The solution was then analyzed using SDS–PAGE (Perfect NT Gel W, 10 to 20% acrylamide, 20 wells; DRC Co., Ltd., Tokyo, Japan) in accordance with the manufacturer's protocol. The gel was stained with Coomassie brilliant blue (CBB) (PhastGel Blue R; GE Healthcare, Little Chalfont, UK). TotalLab TL120 software v2006 (Shimadzu Co.) quantified the intensity of each protein band, and the intensity was used as an index of the level of protein expression. The protein bands were excised from the gel; in-gel tryptic digestion was performed and the protein was identified, as we previously described (Hattori et al., 2009).

Western Blotting

The protein extracts were separated by electrophoresis on 10 to 20% gradient gels (DRC Co., Ltd.). The proteins were transferred to polyvinylidene fluoride membranes (Millipore Corporate Headquarters, Billerica, MA) in a tank-transfer apparatus (Bio-Rad Laboratories, Hercules, CA). The membranes were blocked with 5% skim milk in phosphate-buffered saline (PBS). Mouse anti-PEDF (TransGenic Inc., Hyogo, Japan) diluted 1:250 in blocking buffer was used as the primary antibody. Peroxidase-conjugated AffiniPure goat anti-mouse IgG (H+L) (Jackson ImmunoResearch Laboratories Inc., West Grove, PA) diluted 1:1,000 in blocking buffer was used as the secondary antibody. Enhanced chemiluminescence detection reagents (GE Healthcare, Buckinghamshire, UK) detected the antigens on the membrane. TotalLab TL120 software v2006 (Shimadzu Co.) quantified the intensity of each protein band; the intensity was used as an index of the level of protein expression.

Other Procedures

Serum levels of PEDF were determined by enzyme-linked immunosorbent assay (ELISAquant™ PEDF Sandwich ELISA Antigen Detection Kit [BioProducts MD, Middletown, MD]). Numerical data are presented as the mean ± standard deviation (SD). We evaluated the statistical significance using IBM SPSS Statistics 18 software (SPSS Inc., Chicago, IL). p Values less than 0.05 were considered significant.

RESULTS

Three-Step Proteome Analyses

Two serum samples from each of the 8 patients with alcohol abuse—one sample obtained on admission and the second, after 8 weeks of abstinence—were subjected to three-step serum proteome analysis. A representative CBB-stained SDS–PAGE gel (fraction No. 14) is shown in Fig. 1*A*. After converting the intensity of each band to a numerical value

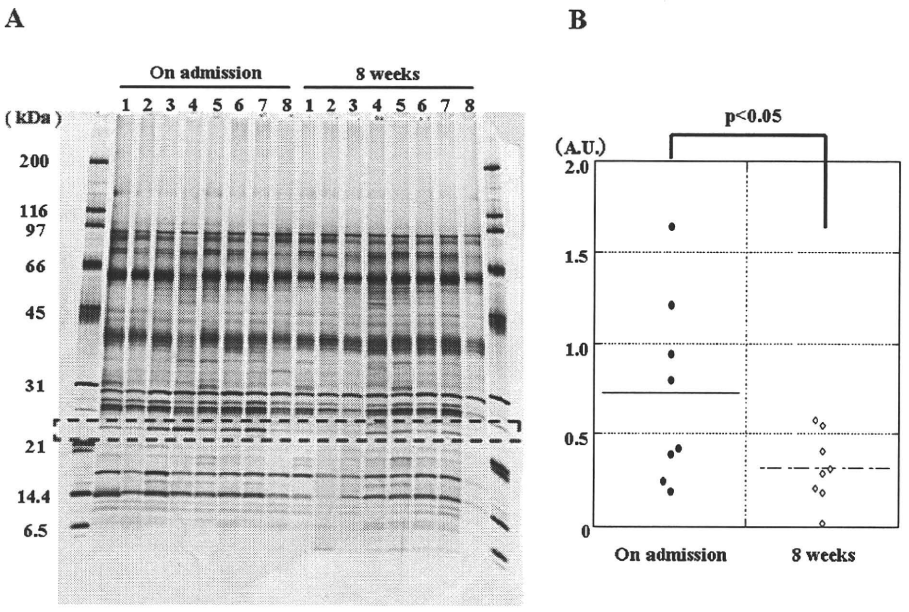

Fig. 1. Representative SDS–PAGE gel of an RP-HPLC fraction (fraction No. 14) and the comparison of the band intensities, as assessed by densitometry. Serum samples (100 μL each) were immunodepleted and injected onto the RP-HPLC column. Proteins in each fraction were subjected to 10 to 20% SDS–PAGE, as described in Methods. Following electrophoresis, the proteins were visualized using CBB staining. The image indicates the 25-kDa band that is equivalent to PEDF (**A**). The expression level of the 25 kDa band was quantified using densitometry in the 8 pairs of samples (i.e., 16 samples). The difference in the PEDF expression level is statistically significant (**B**). CBB, coomassie brilliant blue; ELISA, enzyme-linked immunosorbent assay; PEDF, pigment epithelial-derived factor; RP-HPLC, reverse-phase high-performance liquid chromatography; SDS–PAGE, sodium dodecyl sulfate polyacrylamide gel electrophoresis.

Table 2. Serum Proteins Upregulated (A) and Downregulated (B) in Alcoholic Patients on Admission, as Detected by Three-Step Proteome Analysis

No.	Database accession no.	ID	MW	Score	Number of matching peptides	Sequence coverage (%)
A. Upregulated serum proteins						
1	gi2521981	Alpha2-HS glycoprotein	35,641	112	5	8
2	gi90108664	Apolipoprotein A-I	28,061	1,409	43	70
3	gi121672	Glutathione peroxidase 3	25,489	82	2	6
4	gi23200172	Heparin cofactor II	57,034	161	3	5
5	gi189778	PEDF	46,300	491	9	22
B. Downregulated serum proteins						
1	gi224917	Apolipoprotein C-III	8,759	118	3	24

MW, molecular weight; PEDF, pigment epithelial-derived factor.

(using TotalLab TL120 software v2006), the 8 pairs of samples showed a significant difference in the expression level of the 25 kDa band on admission and after 8 weeks of abstinence from drink ($p < 0.05$) (Fig. 1*B*). A comparison of all 40 RP-HPLC fractions revealed that the expression levels of 27 bands at the time of admission changed significantly after 8 weeks abstinence from drink ($p < 0.01$). On admission, 24 bands were upregulated and three bands were downregulated.

Identification of Protein

Of the 27 bands, 6 bands, which demonstrated particularly remarkable changes, were digested by trypsin and were subjected to tandem mass spectrometry for identification. The 6 proteins that were identified are listed in Table 2. The 5 proteins that were upregulated on admission were alpha2-HS glycoprotein, apolipoprotein A-I, glutathione peroxidase 3, heparin cofactor II, and PEDF (Table 2A). The protein band that was downregulated on admission was apolipoprotein C-III (Table 2B).

Western Blotting

Of the 5 proteins upregulated on admission, we focused on PEDF mainly because the alteration in the levels of this protein because of heavy drinking is not well known. The results obtained by SDS–PAGE were confirmed by Western blotting performed on the same 8 pairs of serum samples subjected to the three-step proteome analysis (Fig. 2*A*). A semiquantitative analysis of the results, using the TotaLab TL120 software, revealed a statistically significant difference between the serum PEDF level on admission and after 8 weeks of abstinence from drink ($p < 0.05$) (Fig. 2*B*).

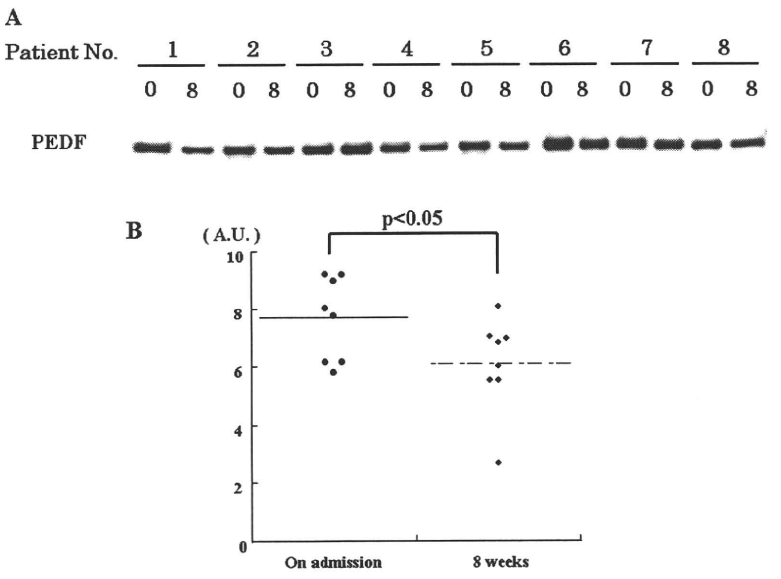

Fig. 2. Western blot analysis of PEDF in the serum samples of the alcoholic patients. (**A**) The 8 sample pairs of the immunodepleted sera, which had been obtained from alcoholic patients on admission (week 0) and after 8 weeks of abstinence (week 8). The serum samples were separated using 10 to 12% SDS–PAGE and probed with anti-PEDF antibody, as described in Methods. (**B**) The densitometric comparison of the bands' intensities. The PEDF expression level is significantly greater on admission than after 8 weeks of abstinence ($p < 0.05$). PEDF, pigment epithelial-derived factor; SDS–PAGE, sodium dodecyl sulfate polyacrylamide gel electrophoresis.

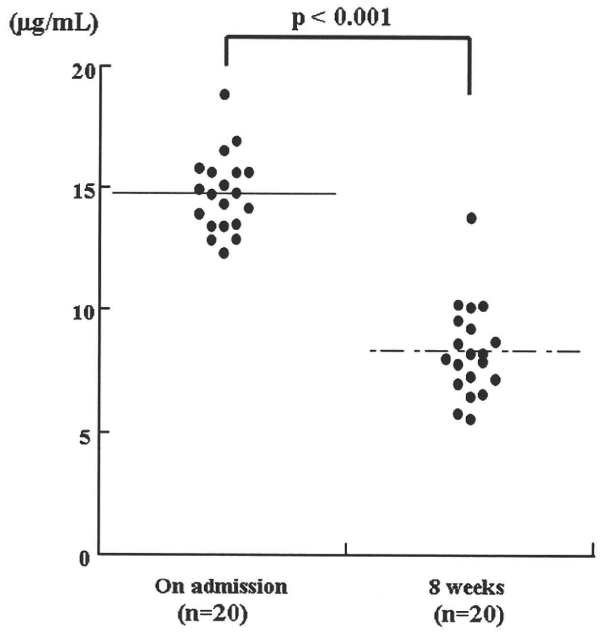

Fig. 3. Serum PEDF levels, as determined by ELISA, in 20 alcoholic patients on admission and after 8 weeks of abstinence. The serum PEDF levels are significantly decreased after 8 weeks of abstinence ($p < 0.001$). ELISA, enzyme-linked immunosorbent assay; PEDF, pigment epithelial-derived factor.

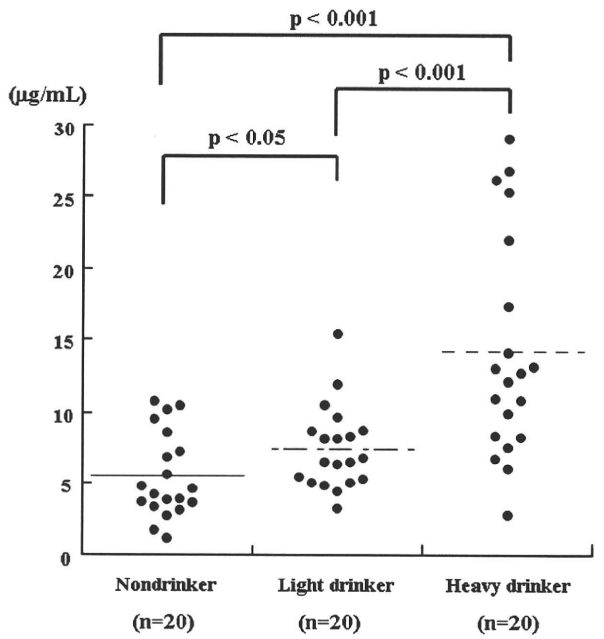

Fig. 4. Serum PEDF levels, as determined by ELISA, in 60 apparently healthy subjects with various drinking habits. The levels are significantly greater in the light habitual drinkers (7.5 ± 2.9 μg/ml) and in the heavy habitual drinkers (14.2 ± 7.7 μg/ml), compared with the nondrinkers (5.5 ± 3.0 μg/ml). ELISA, enzyme-linked immunosorbent assay; PEDF, pigment epithelial-derived factor.

ELISA

ELISA further confirmed an increase in serum PEDF levels in 20 male patients with alcoholic dependency. The PEDF level was 14.6 ± 1.9 μg/ml on admission and decreased significantly to 8.7 ± 2.3 μg/ml after 8 weeks of abstinence from drink ($p < 0.001$) (Fig. 3).

The serum PEDF levels in nondrinkers and habitual drinkers are shown in Fig. 4. The serum PEDF levels in light habitual drinkers (7.5 ± 2.9 μg/ml) and in heavy habitual drinkers (14.2 ± 7.7 μg/ml) were significantly greater than in nondrinkers (5.5 ± 3.0 μg/ml).

Serum PEDF levels were also measured in subjects with nonalcoholic chronic liver diseases of viral and nonviral origin. The PEDF levels in subjects with chronic nonalcoholic liver diseases were comparable to the PEDF levels in normal subjects without a drinking habit, as indicated in Fig. 5.

Serum PEDF levels of the control subjects younger than 50 yrs were 9.4 ± 7.3 μg/ml and the levels in those older than 50 years were 8.7 ± 5.1 μg/ml, indicating that there are no age-related differences in serum PEDF levels. In a total of 120 patients with nonalcoholic liver diseases, there were no gender-related differences (4.2 ± 2.1 μg/ml in males and 4.5 ± 2.4 μg/ml in females).

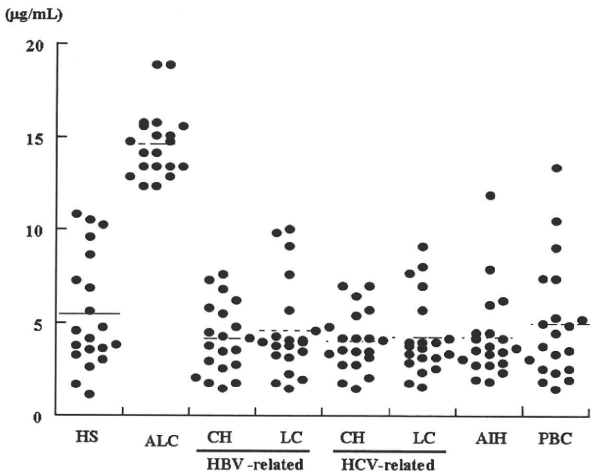

Fig. 5. Serum PEDF levels, as determined by ELISA, in alcoholic patients and in patients with chronic liver diseases of nonalcoholic etiology. The PEDF levels are significantly greater in alcoholic patients than in the healthy subjects. However, the PEDF levels in other patient groups are comparable to those in the healthy controls. AIH, autoimmune hepatitis; ALC, alcohol dependency; CH, chronic hepatitis; ELISA, enzyme-linked immunosorbent assay; HS, healthy subjects; LC, liver cirrhosis; PBC, primary biliary cirrhosis; PEDF, pigment epithelial-derived factor.

DISCUSSION

Recent advances in proteomic technology have provided promising ways to discover and identify novel biomarkers in various fields of clinical medicine. The application of various gel-based and gel-free methods has facilitated the discovery of potential clinical biomarkers, although there has been a long

and uncertain path from marker discovery to clinical utility. We previously discovered a 5.9-kDa peptide as a novel biomarker of alcohol abuse using mass spectrometry–based methods (Nomura et al., 2004; Sogawa et al., 2007). We also used fluorescent two-dimensional difference gel electrophoresis (2D-DIGE) for serum proteome analysis and found a change before and after abstinence in the serum levels of relatively abundant proteins (including alpha 1-antichymotripsin and haptoglobin) in subjects with alcohol abuse (Wu et al., 2007).

A technical challenge in serum proteome analysis has been that serum contains thousands of proteins and peptides that are present in a large dynamic range. Indeed, 22 abundant proteins (e.g., albumin, immunoglobulins, and transferrin) constitute up to 99% of the protein content of plasma (Anderson and Anderson, 2002; Tirumalai et al., 2003). Depletion of these abundant proteins and further fractionation of samples will be necessary in future proteomic studies searching for low-abundant serum proteins or peptides.

We previously used the three-step method and detected 3 proteins, including YKL-50, as promising novel biomarkers of sepsis (Hattori et al., 2009). We assessed reproducibility of the three-step method. To assess between-days precision, 4 aliquots of 40 μl from the same serum samples were subjected to the three-step proteome analyses on 4 different days, and silver-stained SDS–PAGE results of the 4 fractions were compared. As shown in Fig. S1, the between-day differences were minimal. In the present study, we applied the three-step method to search for biomarkers for excessive alcohol drinking. We performed three-step proteome analysis on 2 serum samples collected from each of 8 patients (16 samples in total) with alcohol dependence—one sample was collected on admission and one sample was collected after 8 weeks of abstinence from drink. Three-step serum proteome analysis revealed that the serum levels of 5 proteins—alpha2-HS glycoprotein, apolipoprotein A-I, glutathione peroxidase 3, heparin cofactor II, and PEDF were significantly greater on admission than after 8 weeks of abstinence. On the other hand, serum levels of apolipoprotein III were downregulated on admission. Although the data were shown only for PEDF, the results of Western blotting confirmed the changes in the expression levels of all the 6 proteins by heavy drinking. As alterations of serum levels of apolipoprotein A-I, alpha-2-HS glycoprotein, apolipoprotein C-III, glutathione peroxidase 3, and heparin cofactor II associated excessive alcohol consumption have been reported in the literature (Andersson and Bell, 1988; Kaku et al., 1982; Nanchahal et al., 2000; Peng et al., 2005; Robinson and Quarfordt, 1981), we focused on PEDF, alterations of which by heavy drinking are not well characterized. In the present study, these changes were initially detected by SDS–PAGE, the final step of the three-step proteome analysis. Western blotting and ELISA further confirmed these changes. After patients with alcohol abuse abstained from alcohol for 2 months, their elevated serum PEDF levels (noted on admission) returned to the levels found in the control subjects. This suggests that active and excessive drinking, rather than liver injury per se, could play a role in the upregulation of PEDF.

This notion is partially supported by data showing that the serum PEDF levels in people with nonalcoholic chronic liver diseases, including liver cirrhosis, are comparable to the serum PEDF levels in normal controls without a drinking history. Furthermore, serum PEDF levels in habitual drinkers are significantly greater than serum PEDF levels in nondrinkers.

PEDF is a glycoprotein belonging to the serine protease inhibitor superfamily. It was originally purified from the culture supernatant of retinal pigment epithelial cells as a factor that inhibited vascularization (Leung et al., 1989) and exhibited potent neurosecretory activity for human retinoblastoma cells (Tombran-Tink et al., 1991). The PEDF gene contains 8 exons and 7 introns and is located on chromosome 17p13.1. Its transcript is widely expressed in various tissues such as the eye, brain, spinal cord, skeletal muscle, adipose tissue, liver, and bone (Rychli et al., 2009). PEDF is reportedly also present in human plasma at a concentration of around 5 μg/ml (Petersen et al., 2003), which is very similar to the levels obtained in normal controls without drinking history in the present study.

Serum or plasma PEDF levels have been determined in several pathological conditions. Plasma PEDF levels are significantly elevated in diabetic patients, especially in patients with proliferative diabetic retinopathy (Ogata et al., 2007). Elevated serum levels of PEDF in metabolic syndrome have also been reported (Yamagishi et al., 2006). Matsumoto and colleagues (2004) measured serum PEDF levels in various chronic liver diseases. They reported that serum PEDF levels in patients with liver cirrhosis because of hepatitis C virus are significantly lower than the serum PEDF in controls subjects. These results do not agree with the findings of this study. The reasons for this discrepancy are not clear at the moment. It should be noted, however, that Matsumoto and colleagues used a particular ELISA kit from Chemicon International, which is good for measuring the PEDF level of vitreous fluid, but is reportedly not appropriate for measuring the serum PEDF level (Yamagishi et al., 2006). Indeed, the PEDF levels in the controls in Matsumoto's study were around 6 ng/ml, which is lower by almost three-orders magnitude than the levels obtained in this study (5 μg/ml).

The biological significance of the increase in serum PEDF after excessive alcohol drinking is of great interest. In this context, the antiangiogenic, antitumorigenic, antioxidant, antithrombotic, and anti-inflammatory properties of PEDF have to be considered (Rychli et al., 2009; Tombran-Tink and Barnstable, 2003; Uehara et al., 2004; Yamagishi et al., 2009). It has recently been suggested that PEDF plays a protective role in atherosclerosis and that the antiatherothrombogenic property of PEDF may be a therapeutic target in cardiovascular disease (Rychli et al., 2009; Yamagishi and Matsui, 2010). The reduced risk of fatal coronary diseases in habitual drinkers is well documented, but the underlying

mechanisms are complex (Renaud et al., 2004). It is tempting to speculate that the upregulation of PEDF may (at least partly) play a role in this protective action. Thus, three-step serum proteome analysis reveals that serum PEDF levels are significantly increased after excessive drinking. The exact diagnostic and pathophysiological roles of this phenomenon remain to be investigated.

GRANT SUPPORT

Ministry of Education, Culture, Science, Sports, and Technology of Japan.

REFERENCES

Alling C, Chick JD, Anton R, Mayfield RD, Salaspuro M, Helander A, Harris RA (2005) Revealing alcohol abuse: to ask or to test? Alcohol Clin Exp Res 29:1257–1263.

Anderson NL, Anderson NG (2002) The human plasma proteome: history, character, and diagnostic prospects. Mol Cell Proteomics 1:845–867.

Andersson TR, Bell H (1988) Plasma heparin cofactor II in alcohol liver disease. J Hepatol 7:79–84.

Conigrave KM, Degenhardt LJ, Whitfield JB, Saunders JB, Helander A, Tabakoff B (2002) CDT, GGT, and AST as markers of alcohol use: the WHO/ISBRA collaborative project. Alcohol Clin Exp Res 26:332–339.

Hannuksela ML, Liisanantti MK, Nissinen AE, Savolainen MJ (2007) Biochemical markers of alcoholism. Clin Chem Lab Med 45:953–961.

Hattori N, Oda S, Sadahiro T, Nakamura M, Abe R, Shinozaki K, Nomura F, Tomonaga T, Matsushita K, Kodera Y, Sogawa K, Satoh M, Hirasawa H (2009) YKL-40 identified by proteomic analysis as a biomarker of sepsis. Shock 32:393–400.

Kaku Y, Hasumura Y, Takeuchi J (1982) Clinical detection of the hepatic lesion of pericentral sclerosis in chronic alcoholics. Gut 23:215–220.

Kawashima Y, Fukuno T, Satoh M, Takahashi H, Matsui T, Maeda T, Kodera Y (2009) A simple and highly reproducible method for discovering potential disease markers in low abundance serum proteins. J Electrophor 53:13–18.

Leung DW, Cachianes G, Kuang WJ, Goeddel DV, Ferrara N (1989) Vascular endothelial growth factor is a secreted angiogenic mitogen. Science 246:1306–1309.

Matsumoto K, Ishikawa H, Nishimura D, Hamasaki K, Nakao K, Eguchi K (2004) Antiangiogenic property of pigment epithelium-derived factor in hepatocellular carcinoma. Hepatology 40:252–259.

Nanchahal K, Ashton WD, Wood DA (2000) Alcohol consumption, metabolic cardiovascular risk factors and hypertension in women. Int J Epidemiol 29:57–64.

Niemela O (2007) Biomarkers in alcoholism. Clin Chim Acta 377:39–49.

Nomura F, Tomonaga T, Sogawa K, Ohashi T, Nezu M, Sunaga M, Kondo N, Iyo M, Shimada H, Ochiai T (2004) Identification of novel and down-regulated biomarkers for alcoholism by surface enhanced laser desorption/ionization-mass spectrometry. Proteomics 4:1187–1194.

Nomura F, Tomonaga T, Sogawa K, Wu D, Ohashi T (2007) Application of proteomic technologies to discover and identify biomarkers for excessive alcohol consumption: a review. J Chromatogr B Analyt Technol Biomed Life Sci 855:35–41.

Ogata N, Matsuoka M, Matsuyama K, Shima C, Tajika A, Nishiyama T, Wada M, Jo N, Higuchi A, Minamino K, Matsunaga H, Takeda T, Matsumura M (2007) Plasma concentration of pigment epithelium-derived factor in patients with diabetic retinopathy. J Clin Endocrinol Metab 92:1176–1179.

Peng FC, Tang SH, Huang MC, Chen CC, Kuo TL, Yin SJ (2005) Oxidative status in patients with alcohol dependence: a clinical study in Taiwan. J Toxicol Environ Health A 17–18:1497–1509.

Petersen SV, Valnickova Z, Enghild JJ (2003) Pigment-epithelium-derived factor (PEDF) occurs at a physiologically relevant concentration in human blood: purification and characterization. Biochem J 15:199–206.

Renaud S, Lanzmann-Petithory D, Gueguen R, Conard P (2004) Alcohol and mortality from all causes. Biol Res 37:183–187.

Robinson SF, Quarfordt SH (1981) The effect of ethanol on lipoprotein metabolism. Alcohol Clin Exp Res 5:101–109.

Rychli K, Huber K, Wojta J (2009) Pigment epithelium-derived factor (PEDF) as a therapeutic target in cardiovascular disease. Expert Opin Ther Targets 13:1295–1302.

Sogawa K, Itoga S, Tomonaga T, Nomura F (2007) Diagnostic values of surface-enhanced laser desorption/ionization technology for screening of habitual drinkers. Alcohol Clin Exp Res 31:22S–26S.

Sogawa K, Satoh M, Kodera Y, Tomonaga T, Iyo M, Nomura F (2009) A search for novel markers of alcohol abuse using magnetic beads and MALDI-TOF/TOF mass spectrometry. Proteomics Clin Appl 3:821–828.

Tirumalai RS, Chan KC, Prieto DA, Issaq HJ, Conrads TP, Veenstra TD (2003) Characterization of the low molecular weight human serum proteome. Mol Cell Proteomics 2:1096–1103.

Tombran-Tink J, Barnstable CJ (2003) PEDF: a multifaceted neurotrophic factor. Nat Rev Neurosci 4:628–636.

Tombran-Tink J, Chader CG, Johnson LV (1991) PEDF: pigment epithelium-derived factor with potent neuronal differentiative activity. Exp Eye Res 53:411–414.

Uehara H, Miyamoto M, Kato K, Ebihara Y, Kaneko H, Hashimoto H, Murakami Y, Hase R, Takahashi R, Mega S, Shichinohe T, Kawarada Y, Itoh T, Okushiba S, Kondo S, Katoh H (2004) Expression of pigment epithelium-derived factor decreases liver metastasis and correlates with favorable prognosis for patients with ductal pancreatic adenocarcinoma. Cancer Res 64:3533–3537.

Umemura H, Nezu M, Kodera Y, Satoh M, Kimura A, Tomonaga T, Nomura F (2009) Effects of the time intervals between venipuncture and serum preparation for serum peptidome analysis by matrix-assisted laser desorption/ionization time-of-flight mass spectrometry. Clin Chim Acta 406:179–180.

Wu D, Tomonaga T, Sogawa K, Satoh M, Sunaga M, Nezu M, Oh-Ishi M, Kodera Y, Maeda T, Ochiai T, Nomura F (2007) Detection of biomarkers for alcoholism by two-dimensional differential gel electrophoresis. Alcohol Clin Exp Res 31:67S–71S.

Yamagishi S, Adachi H, Abe A, Yashiro T, Enomoto M, Furuki K, Hino A, Jinnouchi Y, Takenaka K, Matsui T, Nakamura K, Imaizumi T (2006) Elevated serum levels of pigment epithelium-derived factor in the metabolic syndrome. J Clin Endocrinol Metab 91:2447–2450.

Yamagishi S, Matsui T (2010) Anti-atherothrombogenic properties of PEDF. Curr Mol Med 10:284–291.

Yamagishi S, Matsui T, Nakamura K (2009) Atheroprotective properties of pigment epithelium-derived factor (PEDF) in cardiometabolic disorders. Curr Pharm Des 15:1027–1033.

SUPPORTING INFORMATION

Additional Supporting Information may be found in the online version of this article:

Fig. S1. Silver-stained SDS–PAGE shows the reproducibility of the method. Four aliquots of 40 μl from the same serum sample underwent the three-step method. One-sixteenth of each sample (corresponding to the proteins from 2.5 μl serum) is loaded in each lane. SDS–PAGE, sodium dodecyl sulfate polyacrylamide gel electrophoresis

Please note: Wiley-Blackwell is not responsible for the content or functionality of any supporting information supplied by the authors. Any queries (other than missing material) should be directed to the corresponding author for the article.

Journal of Medical Virology 83:201–207 (2011)

Hepatitis A Viral Load in Relation to Severity of the Infection

Keiichi Fujiwara,[1]* Hiroshige Kojima,[1] Shin Yasui,[1] Koichiro Okitsu,[1] Yutaka Yonemitsu,[1] Masao Omata,[2] and Osamu Yokosuka[1]

[1]*Department of Medicine and Clinical Oncology, Graduate School of Medicine, Chiba University, Chiba, Japan*
[2]*Department of Gastroenterology, University of Tokyo, Tokyo, Japan*

A correlation between hepatitis A virus (HAV) genomes and the clinical severity of hepatitis A has not been established. The viral load in sera of hepatitis A patients was examined to determine the possible association between hepatitis A severity and HAV replication. One hundred sixty-four serum samples from 91 Japanese patients with sporadic hepatitis A, comprising 11 patients with fulminant hepatitis, 10 with severe acute hepatitis, and 70 with self-limited acute hepatitis, were tested for HAV RNA. The sera included 83 serial samples from 20 patients. Viral load was measured by real-time RT-PCR. The detection rates of HAV RNA from fulminant, severe acute, and acute hepatitis were 10/11 (91%), 10/10 (100%), and 55/70 (79%), respectively. Mean values of HAV RNA at admission were 3.48 ± 1.30 logcopies/ml in fulminant, 4.19 ± 1.03 in severe acute, and 2.65 ± 1.64 in acute hepatitis. Patients with severe infection such as fulminant hepatitis and severe acute hepatitis had higher initial viral load than patients with less severe infection ($P < 0.001$). Viremia persisted for 14.2 ± 5.8 days in patients with severe infection and 21.4 ± 10.6 days in those with acute hepatitis after clinical onset ($P = 0.19$). HAV RNA was detectable quantitatively in the majority of the sera of hepatitis A cases during the early convalescent phase by real-time PCR. Higher initial viral replication was found in severely infected patients. An excessive host immune response might follow, reducing the viral load rapidly as a result of the destruction of large numbers of HAV-infected hepatocytes, and in turn severe disease might be induced. ***J. Med. Virol. 83:201–207, 2011.*** © 2010 Wiley-Liss, Inc.

KEY WORDS: hepatitis A; fulminant hepatitis; severe acute hepatitis; hepatitis A virus; real-time PCR

INTRODUCTION

Hepatitis A virus (HAV) is a major etiologic agent of acute hepatitis, and it still poses a considerable problem worldwide. HAV causes self-limited acute hepatitis in most cases, but fulminant hepatitis develops in 0.1–0.2% of the cases.

Although the virological aspects of HAV have been studied extensively, a correlation between viral characteristics and clinical severity has still not been demonstrated. A sensitive nested RT-PCR method was therefore developed to detect serum HAV RNA in the early convalescent phase of hepatitis A with high frequency [Fujiwara et al., 1997], and the viral genomes in the sera from hepatitis A patients with a variety of clinicopathological features were analyzed and the associations between certain viral regions and clinical severities were documented. It has been reported that both viral and host factors should be considered when discussing the mechanisms responsible for the severity of hepatitis A [Fujiwara et al., 2000, 2001, 2002], and that several portions of the HAV genome including the 5′ non-translated region (5′NTR) and non-structural protein 2B and 2C [Fujiwara et al., 2003, 2007a,b, 2009], whose mutations have been shown to be important for enhanced replication and virulence in cell culture systems [Zhang et al., 1995] and simians [Raychaudhuri et al., 1998], should be examined.

The association between the severity of hepatitis A and serum HAV load has not yet been established because of the nature of acute illness and the difficulty of HAV quantitation [Fujiwara et al., 2005, 2009]. In the

Disclosures: All authors have nothing to disclose.

*Correspondence to: Keiichi Fujiwara, MD, PhD, Department of Medicine and Clinical Oncology, Graduate School of Medicine, Chiba University, 1-8-1 Inohana, Chuo-ku, Chiba 260-8670, Japan. E-mail: fujiwara-cib@umin.ac.jp

Accepted 23 August 2010
DOI 10.1002/jmv.21958
Published online in Wiley Online Library (wileyonlinelibrary.com).

present study, HAV load and viremia of serial serum samples were examined during various clinical courses of hepatitis A both qualitatively and quantitatively by real-time RT-PCR method in an attempt to determine the association between severity of hepatitis A and HAV replication.

PATIENTS AND METHODS

Patients

One hundred sixty-four serum samples were obtained from 91 Japanese patients with sporadic hepatitis A recruited at six university hospitals located in various regions of Japan, comprising 11 patients with fulminant hepatitis, 10 with severe acute hepatitis, and 70 with self-limited acute hepatitis. The sera were collected between 1990 and 2002. They were kept at 100 μl per tube and stored at −20°C until analysis. Among them were 83 serial serum samples from 20 patients, 3 with fulminant hepatitis, 4 with severe acute hepatitis, and 13 with acute hepatitis. These patients were diagnosed on the basis of IgM anti-HAV antibody (IgM-HA) positivity in conjunction with compatible symptoms and laboratory findings. Informed consent was obtained from patients or appropriate family members. The study protocol conformed to the ethical guidelines of the 1975 Declaration of Helsinki as reflected in a priori approval by the appropriate institutional review committee.

Patients with prothrombin time (PT) <40% but without hepatic encephalopathy were defined as severe acute hepatitis, and those with hepatic encephalopathy as fulminant hepatitis. IgM anti-HBc antibody (IgM-HBc), HBsAg, and second-generation anti-HCV antibody were examined in all cases. HCV RNA, IgM anti-Epstein–Barr virus antibody (IgM-EBV), IgM anti-herpes simplex virus antibody (IgM-HSV), IgM anti-cytomegalovirus antibody (IgM-CMV), anti-smooth muscle antibody, liver kidney microsomal antibody-1 and anti-mitochondrial antibody were also examined in patients with fulminant hepatitis and severe acute hepatitis as well as in some patients with acute hepatitis showing an atypical course. In addition, histories of recent exposure to drugs and chemical agents as well as of heavy alcohol consumption (>50 g/day for >5 years) were examined. None of the patients had clinical or laboratory evidence of acquired immune deficiency syndrome.

In hepatitis A, early symptoms including fever, general malaise, fatigue, nausea, vomiting and right upper quadrant discomfort are frequently observed, so we defined the beginning of these symptoms as clinical onset.

Serological markers

IgM-HA, IgM-HBc antibody, and HBsAg were measured by commercial radioimmunoassay kits (Abbott Laboratories, Chicago, IL), and second-generation HCV antibody was measured by enzyme immunoassay kit (Ortho Diagnostics, Tokyo, Japan). In fulminant hepatitis and severe acute hepatitis, HCV RNA was measured by nested RT-PCR. IgM-EBV, IgM-CMV, and IgM-HSV were examined by enzyme-linked immunosorbent assays, and anti-nuclear antibody, anti-smooth muscle antibody, anti-mitochondrial antibody, and anti-liver kidney microsomal antibody-1 were examined by fluorescent antibody method.

Quantitation of HAV RNA by Real-Time RT-PCR

Serum viral RNA was extracted using a High Pure Viral RNA Kit (Roche Diagnostics GmbH, Mannheim, Germany). One-step RT-PCR was carried out with a Hepatitis A Virus Quantification Kit (Roche Diagnostics GmbH) according to the manufacturer's instructions, which enable quantitation of RNA encoding HAV and simultaneous detection of HAV-specific internal control. Briefly, 20 μl of PCR mixture contained 15 μl of master mix from the Hepatitis A Virus Quantification Kit (Roche Diagnostics GmbH) and 5 μl of template RNA solution extracted from 20 μl of serum. LightCycler capillaries were sealed, centrifuged, and transferred to a LightCycler instrument (Roche Diagnostics GmbH). Reverse transcription was done for 10 min at 55°C, followed by 30-sec denaturing at 95°C. The corresponding cDNA was amplified by PCR of 45 cycles at 95°C for 5 sec, 55°C for 15 sec, and 72°C for 12 sec. The HAV RNA standards come supplied with this kit. All reactions were performed in the LightCycler (Roche Diagnostics GmbH). The CT values from clinical samples were plotted on a standard curve, and the number of copies was calculated automatically. This method provides a dynamic range of HAV RNA quantitation between 1.40 and 8.40 logcopies/ml.

Statistical Analysis

Differences in proportions among groups were compared by Fisher's exact probability test, Student's *t*-test, and Welch's *t*-test.

RESULTS

Clinical Characteristics

The characteristics of the 91 patients at admission are summarized in Table I. None of them was epidemic related.

Differences in male-to-female ratio and mean age among fulminant hepatitis, severe acute hepatitis, and acute hepatitis cases were not statistically significant. Mean alanine aminotransferase (ALT) level, mean total bilirubin (T-Bil) level, days from onset to serum sampling and presence of chronic liver disease were not significantly different among fulminant hepatitis, severe acute hepatitis and acute hepatitis cases. Mean PT activity was lower in fulminant hepatitis than in acute hepatitis and severe acute hepatitis and lower in severe acute hepatitis than in acute hepatitis.

Five (45%) of 11 patients with fulminant hepatitis died of hepatic failure, 1 (10%) of 10 with severe acute hepatitis died of sepsis, and all acute hepatitis patients

TABLE I. Characteristics of All Patients at Admission

	Fulminant hepatitis	Severe acute hepatitis	Acute hepatitis
n	11	10	70
Sex (M/F)	5/6[1)]	6/4[1)]	36/34[1)]
Age[a]	43.5 ± 15.2[2)]	40.0 ± 13.2[2)]	40.1 + 11.3[2)]
PT (%)[a]	17 ± 9[3)]	33 ± 8[3)]	75 ± 11[3)]
ALT (IU/L)[a]	5,538 ± 3,528[4)]	5,618 ± 3,186[4)]	4,353 ± 1,592[4)]
T-Bil (mg/dl)[a]	10.1 ± 6.5[5)]	6.0 ± 7.0[5)]	6.0 ± 3.8[5)]
Serum sampling (days from onset)[a]	11.3 ± 9.7[6)]	10.2 ± 10.5[6)]	15.5 ± 17.1[6)]
CLD	2[7)]	1[7)]	4[7)]
Death	5[8)]	1[8)]	0[8)]

PT, prothrombin time; ALT, alanine aminotransferase; T-Bil, total bilirubin; CLD, presence of chronic liver disease.
[1), 2), 4), 5), 6), 7)] Statistically not significant. [3)] Statistically significant between FH and AHs ($P < 0.001$), FH and AH ($P < 0.001$) and AHs and AH ($P < 0.001$) by Student's t-test. [8)] Statistically significant between FH and AH ($P < 0.001$) by Fisher's exact probability test.
[a]Mean ± SD.

recovered. The difference in mortality between fulminant hepatitis and acute hepatitis was statistically significant ($P < 0.001$ by Fisher's exact probability test).

Two patients with acute hepatitis were positive for HBsAg and anti-HBe antibody, and one patient with acute hepatitis was positive for antinuclear antibody but showed a typical hepatitis A clinical course. One patient with acute hepatitis was diagnosed as autoimmune hepatitis triggered by HAV infection. HCV RNA was negative in all patients with fulminant hepatitis and severe acute hepatitis. One patient with fulminant hepatitis was positive for HCV antibody on admission, and this patient had a previously documented HCV infection, although data for previous liver function tests were not available. One with fulminant hepatitis and one with severe acute hepatitis had alcoholic liver disease. IgM-EBV, IgM-HSV, IgM-CMV, anti-nuclear antibody, anti-smooth muscle antibody, liver kidney microsomal antibody-1, and anti-mitochondrial antibody were negative in all examined fulminant hepatitis and severe acute hepatitis patients.

Detection and Quantitation of HAV RNA at Admission

At admission, the detection rates of HAV RNA from fulminant hepatitis, severe acute hepatitis, and acute hepatitis were 10/11 (91%), 10/10 (100%), and 55/70 (79%), respectively. The differences between the respective groups were not significant.

Serum sampling at admission was 10.0 ± 8.6 days after onset in HAV RNA positive cases and 35.2 ± 23.7 days in HAV RNA negative ones, with the difference in timing being significant ($P < 0.001$) (Fig. 1).

The mean values of HAV RNA at admission were 2.92 ± 1.62 logcopies/ml, with 3.48 ± 1.30 logcopies/ml in fulminant hepatitis, 4.19 ± 1.03 in severe acute hepatitis, 3.82 ± 1.20 in fulminant hepatitis and severe

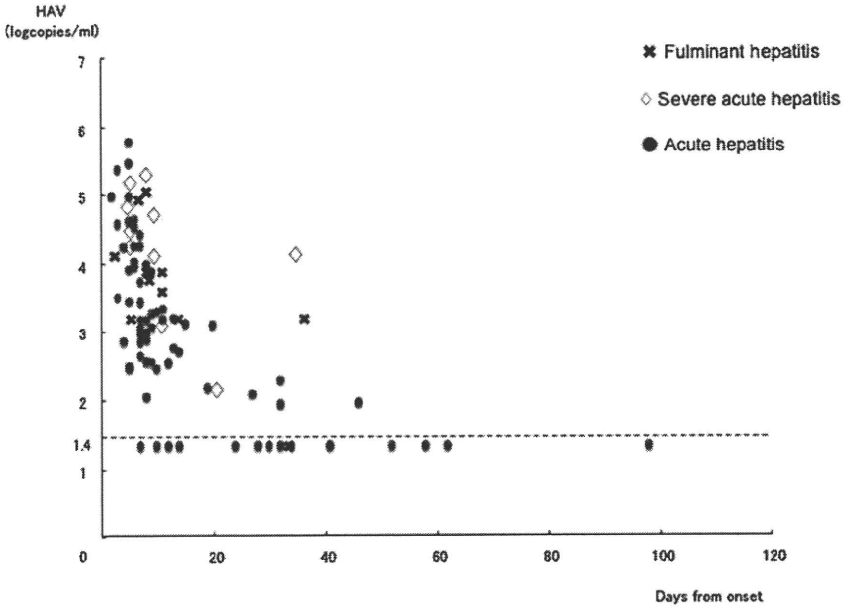

Fig. 1. Association between the duration from onset and initial HAV load in various severities of patients with hepatitis A.